Mergers and Bulge Formation In {lambda}cdm: Which Mergers Matter?

SUBMITTED TO APJ, AUGUST 20, 2009
Preprint typeset using LaTeX style emulateapj v. 11/10/09

MERGERS AND BULGE FORMATION IN ΛCDM: WHICH MERGERS MATTER?

PHILIP F. HOPKINS[1], KEVIN BUNDY[1], DARREN CROTON[2], LARS HERNQUIST[3], DUSAN KERES[3,4], SADEGH KHOCHFAR[5], KYLE STEWART[6], ANDREW WETZEL[1], JOSHUA D. YOUNGER[3,7]

Submitted to ApJ, August 20, 2009

ABSTRACT

We use a suite of semi-empirical models to predict the galaxy-galaxy merger rate and relative contributions to bulge growth as a function of mass (both halo and stellar), redshift, and mass ratio. The models use empirical constraints on the halo occupation distribution, evolved forward in time, to robustly identify where and when galaxy mergers occur. Together with the results of high-resolution merger simulations, this allows us to quantify the relative contributions of mergers with different properties (e.g. mass ratios, gas fractions, redshifts) to the bulge population. We compare with observational constraints, and find good agreement. We also provide useful fitting functions and make public a code[a] to reproduce the predicted merger rates and contributions to bulge mass growth. We identify several robust conclusions. (1) Major mergers dominate the formation and assembly of $\sim L_*$ bulges and the total spheroid mass density, but minor mergers contribute a non-negligible $\sim 30\%$. (2) This is mass-dependent: bulge formation and assembly is dominated by more minor mergers in lower-mass systems. In higher-mass systems, most bulges originally form in major mergers near $\sim L_*$, but assemble in increasingly minor mergers. (3) The minor/major contribution is also morphology-dependent: higher B/T systems preferentially form in more major mergers, with B/T roughly tracing the mass ratio of the largest recent merger; lower B/T systems preferentially form in situ from minor minors. (4) Low-mass galaxies, being gas-rich, require more mergers to reach the same B/T as high-mass systems. Gas-richness dramatically suppresses the absolute efficiency of bulge formation, but does not strongly influence the relative contribution of major versus minor mergers. (5) Absolute merger rates at fixed mass ratio increase with galaxy mass. (6) Predicted merger rates agree well with those observed in pair and morphology-selected samples, but there is evidence that some morphology-selected samples include contamination from minor mergers. (7) Predicted rates also agree with the integrated growth in bulge mass density with cosmic time, but with factor ~ 2 uncertainty in both – up to half the bulge mass density could come from non-merger processes. We systematically vary the model assumptions, totaling $\sim 10^3$ model permutations, and quantify the resulting uncertainties. Our conclusions regarding the importance of different mergers for bulge formation are very robust to these changes. The absolute predicted merger rates are systematically uncertain at the factor ~ 2 level; uncertainties grow at the lowest masses and high redshifts.

Subject headings: galaxies: formation — galaxies: evolution — galaxies: active — cosmology: theory

1. INTRODUCTION

In the now established ΛCDM cosmology, structure grows hierarchically (e.g. White & Rees 1978), making mergers an inescapable element in galaxy formation. Thirty years ago, Toomre (1977) proposed the "merger hypothesis," that major mergers between spirals could result in elliptical galaxies, and the combination of detailed observations of recent merger remnants (Schweizer 1982; Lake & Dressler 1986; Doyon et al. 1994; Shier & Fischer 1998; James et al. 1999; Genzel et al. 2001; Tacconi et al. 2002; Dasyra et al. 2006, 2007; Rothberg & Joseph 2004, 2006a; van Dokkum 2005) and e.g. faint shells and tidal features around ellipticals (Malin & Carter 1980, 1983; Schweizer 1980; Schweizer & Seitzer 1992; Schweizer 1996) have lent considerable support to this picture (e.g. Barnes & Hernquist 1992).

Mergers are also linked to starburst galaxies and luminous quasars. By exciting tidal torques that lead to rapid inflows of gas into the centers of galaxies (Barnes & Hernquist 1991, 1996), mergers provide the fuel to power intense starbursts (Mihos & Hernquist 1994b, 1996), to feed rapid black hole growth (Di Matteo et al. 2005; Hopkins et al. 2005b,a), and, through various associated feedback channels, convert blue, star-forming galaxies into quiescent, red ones (e.g. Springel et al. 2005a,b). Mergers are inevitably associated with the most luminous star-forming systems, from ULIRGs in the local Universe (Soifer et al. 1984a,b; Joseph & Wright 1985; Sanders & Mirabel 1996) to bright sub-millimeter galaxies at high redshifts (Alexander et al. 2005; Younger et al. 2008b; Shapiro et al. 2008; Tacconi et al. 2008), and properties ranging from their observed kinematics, structural correlations, and clustering link these populations to massive ellipticals today (Lake & Dressler 1986; Doyon et al. 1994; Shier & Fischer 1998; James et al. 1999; Genzel et al. 2001; Rothberg & Joseph 2006a,b; Hopkins et al. 2007d).

Observations have similarly linked mergers to at least

[1] Department of Astronomy, University of California Berkeley, Berkeley, CA 94720, USA
[2] Centre for Astrophysics & Supercomputing, Swinburne University of Technology, P.O. Box 218, Hawthorn, VIC 3122, Australia
[3] Harvard-Smithsonian Center for Astrophysics, 60 Garden Street, Cambridge, MA 02138, USA
[4] W. M. Keck Postdoctoral Fellow at the Harvard-Smithsonian Center for Astrophysics
[5] Max Planck Institut für Extraterrestrische Physik, Giessenbachstr., D-85748, Garching, Germany
[6] Center for Cosmology, Department of Physics and Astronomy, The University of California at Irvine, Irvine, CA 92697, USA
[7] Hubble Fellow, Institute for Advanced Study, Einstein Drive, Princeton, NJ 08540, USA
[a] http://www.cfa.harvard.edu/~phopkins/Site/mergercalc.html

some of the quasar population (Sanders et al. 1988; Canalizo & Stockton 2001; Guyon et al. 2006; Dasyra et al. 2007; Bennert et al. 2008). Although the precise role of mergers is debated, the existence of tight correlations between black hole mass and spheroid properties such as stellar mass (Magorrian et al. 1998), velocity dispersion (Ferrarese & Merritt 2000; Gebhardt et al. 2000), and binding energy (Hopkins et al. 2007c,b; Aller & Richstone 2007; Younger et al. 2008a) imply that the growth of black holes, dominated by bright quasar phases (Soltan 1982; Salucci et al. 1999; Yu & Tremaine 2002; Hopkins et al. 2007e; Shankar et al. 2009), is fundamentally linked to the growth of spheroids.

Despite the importance of galaxy mergers, the galaxy-galaxy merger rate and its consequences remain the subject of considerable theoretical and observational debate. Halo-halo merger rates have been increasingly well-determined with improvements to high-resolution dark matter only simulations, with different groups and simulations yielding increasingly consistent results (see e.g. Gottlöber et al. 2001; Stewart et al. 2008, 2009a; Fakhouri & Ma 2008b; Wetzel et al. 2009a; Genel et al. 2008). But mapping halo-halo mergers to galaxy-galaxy mergers is non-trivial, and there are a number of apparent disagreements in the literature (both theoretical and observational) over the absolute rate of galaxy mergers as a function of galaxy mass and merger mass ratio. Moreover, although most of the literature has focused on the most violent events (major mergers), various high-resolution simulations have shown that a sufficiently large number of minor mergers (in a sufficiently short period of time) can do as much to build bulge[8] mass as a smaller number of major mergers (Naab & Burkert 2003; Bournaud et al. 2005; Younger et al. 2008a; Cox et al. 2008; Hopkins et al. 2009b). So it remains a subject of debate whether or not minor mergers are important for (or may even dominate) bulge formation. Indeed, several questions arise. What is the galaxy-galaxy merger rate as a function of mass ratio, galaxy mass, and redshift? Which mergers – major or minor – are most important to bulge formation? Is this a function of galaxy mass and/or bulge-to-disk ratio? What is the typical merger history through which most of the bulge mass (and, by implication, black hole mass) in the Universe was assembled? What room does this leave for secular or non-merger related processes?

The relative importance of mergers of different mass ratios is critical for understanding the structure of spheroids and the related processes above. Although, in principle, a sufficiently large number of minor mergers could build the same absolute bulge mass as a couple of major mergers, various simulations have shown that the two scenarios produce very different structural properties in the remnants, including rotation and higher-order kinematics, flattening and isophotal shapes, profile shapes, central densities, effective radii, and triaxialities (Weil & Hernquist 1994, 1996; Burkert et al. 2008; Naab et al. 2009; Hoffman et al. 2009). Sufficiently minor mergers may not even preferentially form elliptical-like "classical" bulges, but rather disk-like "pseudo-bulges," which have typically been associated with secular (non-merger) processes (Younger et al. 2008a; Eliche-Moral et al. 2008). These different channels clearly imply dramatically different formation timescales and histories, also important for understanding the star formation histories, stellar populations, colors, abundances and α-enrichment of spheroids, and their gradients (see e.g. Mihos & Hernquist 1994a; Hopkins et al. 2009a; Ruhland et al. 2009; Foster et al. 2009).

Basic questions such as whether or not individual galaxies move continuously in small increments in the Hubble diagram, or can change types significantly, depend on the kind of mergers in which they form. Clearly, if e.g. small bulges in late-type disks are preferentially formed in early major mergers that destroy the disk (a new disk being later accreted), or if they form in situ in minor mergers that only partially affect the disk, the implications for their evolution and the demographics of bulges and disks are substantial. Moreover, to the extent that starburst and/or AGN activity are coupled to bulge formation in mergers, the magnitude, duty cycles, and cosmological evolution of these events is clearly directly linked to the kinds of mergers triggering activity – one would expect continuous, high-duty cycle but low-level activity from sufficiently minor mergers, with more dramatic, dusty, shorter duty-cycle activity in major mergers (Hopkins & Hernquist 2006, 2009; Hopkins et al. 2009d). Whether or not observations could, in principle, see evidence of merger-induced activity in these systems also depends on the kinds of mergers that dominate bulge formation, as does the question of whether or not every bulge/massive elliptical passed through a ULIRG/quasar phase in its formation.

Conditions are ripe to address these questions. In addition to the convergence in theoretical predictions of the halo-halo merger rate, observations have greatly improved constraints on halo occupation statistics: namely, the stellar mass distributions of galaxies hosted by a halo/subhalo of a given mass. Observational constraints from various methods yield consistent results with remarkably small scatter (discussed below), and have been applied from redshifts $z = 0 - 4$ (albeit with increasing uncertainties at higher redshifts). Furthermore, to lowest order, many of the most salient properties for this application appear to depend primarily on halo mass. That is, at fixed $M_{\rm halo}$ other properties such as redshift, environment, color, satellite/central galaxy status, or morphology have a minor impact (see e.g. Yan et al. 2003; Zentner et al. 2005; Tinker et al. 2005; Cooray 2005; Weinmann et al. 2006a; van den Bosch et al. 2007; Conroy et al. 2007; Zheng et al. 2007), the dependence of these properties on mass and one another all being expected consequences of a simple halo occupation distribution. Populating well-determined halo mergers with well-constrained galaxy properties can yield predictions for the galaxy-galaxy merger rate without reference to any (still uncertain) models of galaxy formation and with small uncertainties (as demonstrated in Stewart et al. 2009a). Meanwhile, numerical simulations are beginning to converge in predicting how the efficiency of bulge formation scales with merger mass ratio and other basic parameters (orbital parameters, gas fractions, etc.), making it possible to robustly predict how much bulge should be formed by each event in a given merger history.

In this paper, we present a simple, empirical model using this approach to predict galaxy-galaxy merger rates, and the relative contribution of mergers as a function of mass ratio, each as a function of galaxy mass, redshift, and other properties. We compare variations to the modeling within the range permitted by theory and observations, and show that the questions above can be answered in a robust, largely empirical

[8] In this paper, we take "bulge" to refer to classical spheroids (Sersic index $\gtrsim 2$, somewhat dispersion-supported spheroids), which are believed to primarily form in mergers, unless otherwise specified. We also use the term "bulge" to refer to any classical spheroid – small bulges in disks through S0 and elliptical galaxies.

fashion, and without reference to specific models of galaxy formation.

In § 2 & § 3, we outline the semi-empirical model adopted and show how observed halo occupation constraints lead to galaxy-galaxy merger rates. In § 4 we use this semi-empirical model to predict galaxy-galaxy merger rates as a function of mass ratio, galaxy stellar mass, and redshift. In § 5 we use these predicted merger rates together with the results of high-resolution simulations to identify the relative importance of different mergers as a function of mass ratio, mass, and redshift. In § 6, we extensively vary the model parameters to test the robustness of these conclusions. In § 7, we summarize our conclusions.

Except where otherwise specified, we adopt a WMAP5 cosmology with $(\Omega_{\rm M}, \Omega_{\Lambda}, h, \sigma_8, n_s)$= $(0.274, 0.726, 0.705, 0.812, 0.96)$ (Komatsu et al. 2009) and a Chabrier (2003) IMF, and appropriately normalize all observations and models shown. The choice of IMF systematically shifts the normalization of stellar masses herein, but does not otherwise change our comparisons.

Throughout, we use the notation $M_{\rm gal}$ to denote the baryonic (stellar+cold gas) mass of galaxies; the stellar, cold gas, and dark matter halo masses are denoted M_*, $M_{\rm gas}$, and $M_{\rm halo}$, respectively. When we refer to merger mass ratios, we use the same subscripts to denote the relevant masses used to define a mass ratio (e.g. $\mu_{\rm gal} = M_{\rm gal,2}/M_{\rm gal,1}$), always defined such that $0 < \mu < 1$ ($M_{\rm gal,1} > M_{\rm gal,2}$).

2. THE SEMI-EMPIRICAL MODEL

In order to track merger histories with as few assumptions as possible, we construct the following semi-empirical model, motivated by the halo occupation framework. Essentially, we assume galaxies obey observational constraints on disk masses and gas fractions, and then predict the properties of merger remnants. The model is described in greater detail in Hopkins et al. (2009g), and a similar variant based on subhalo mergers presented in detail in Hopkins et al. (2008d,b), but we summarize the key properties here.

Note that what we describe here is our "default" model. In § 6, we will systematically vary *every* part of this model, and show that our conclusions are robust.

2.1. *Step 1: The Halo+Subhalo Mass Function*

At a given redshift we initialize the halo+subhalo population, onto which we will "paint" galaxies. We do this following the standard Sheth et al. (2001) mass function, calibrated to match the output of high-resolution N-body simulations. Note that the *total* halo mass function (which is what we use to map central galaxy stellar mass to primary halo mass) is nearly identical to the halo+subhalo mass function – as such, including the subhalos explicitly at this stage (which we can do following the fits or methodology in e.g. Vale & Ostriker 2006; Gao et al. 2004; Nurmi et al. 2006; van den Bosch et al. 2005) makes almost no difference to any of our results. This choice, and the known $\sim 5\%$ uncertainties in halo mass functions are negligible compared to other uncertainties in our model. We will also, in § 6, consider how systematic changes in the halo MF owing to different cosmological parameters affect our results, and show that the differences are minimal.

This defines a primary halo mass function. There are of course subhalos in each halo – defining the systems that will ultimately merge and therefore be of interest here – but these come in the first place from mergers of other halos, which we will need to model. We describe this below.

2.2. *Step 2: Painting Central Galaxies Onto Halos*

At a given redshift, we use the halo occupation formalism to construct a mock sample of galaxies, each with a parent halo or subhalo. Specifically, we begin with the observed galaxy stellar mass function (MF), which we take as given. Generally, we will be interested in all galaxies (i.e. the total galaxy stellar mass function). But if we wish to specifically identify only gas-rich or star-forming galaxies, we can just use observations that separate the mass function of those galaxies alone (i.e. that of star-forming or "blue" galaxies).[9]

We then assign each galaxy to a halo or subhalo in a simple manner following the standard halo occupation methodology described in Conroy & Wechsler (2009); ensuring, by construction, that the galaxy mass function and galaxy clustering (as a function of stellar mass, galaxy color, and physical scale) is exactly reproduced. This essentially amounts to a simple "rank ordering" procedure, whereby both galaxies and halos+subhalos are rank-ordered in mass[10], and then assigned to one another in a one-to-one fashion.

2.2.1. *Uncertainties in Galaxy Masses and the Mapping*

The observational uncertainties in the galaxy abundance are a potential source of uncertainty in the model, especially at high redshifts. We will therefore consider three different determinations of the total galaxy stellar MF as a function of redshift, in our "default" model (the model is otherwise identical, but will use one or another determination of the MF). Further variations are explored in § 6, as well. These are taken from (1) Conroy & Wechsler (2009) (our "default" choice, when no other is specified), (2) Pérez-González et al. (2008b), and (3) Fontana et al. (2004).

Each of these stellar MFs is directly constrained as a function of redshift out to at least $z > 4$, more than sufficient for our (generally lower-redshift) predictions here. The specific choices are not important – we could just as well use a number of other observations in the literature (e.g. Bundy et al. 2005; Pannella et al. 2006; Franceschini et al. 2006; Borch et al. 2006; Fontana et al. 2006; Brown et al. 2007; Marchesini et al. 2009; Kajisawa et al. 2009). We choose these three because they bracket the extremes in all of these different observations. Specifically, the differences between mass functions (1)-(3) represent the range across all these different samples. Those, in turn, reflect uncertainties owing to a combination of cosmic variance, selection/completeness, and different methods used to determine galaxy stellar masses (which can easily contribute $\sim 0.3-0.5$ dex uncertainties in especially the high-redshift stellar mass measurements; see Moster et al. 2009; Marchesini et al. 2009; Behroozi et al. 2010). The compi-

[9] At $z < 2$, we adopt the measurements of the type-separated galaxy stellar mass functions from Ilbert et al. (2009), if such separation is desired. At redshifts $z > 2$, type-separated MFs are no longer available, so we simply assume all systems are star-forming; however, the fraction of massive galaxies that are "quenched" and red has become sufficiently low by $z = 2$ (and is rapidly falling) that it makes little difference (e.g. adopting the upper limit – that the red fraction at all masses at $z > 2$ is equal to that at $z = 2$ – makes no difference to our predictions).

[10] In what follows, the term "mass" of a subhalo will always, unless otherwise specified, refer to the "infall" or maximum mass of the subhalo, pre-accretion (i.e. the maximum mass the system had while it was still a primary halo, before being accreted and becoming a subhalo). This is what is important for the galaxy properties, and what enters into the HOD rank-ordering methodology. Obviously, at a later time after accretion, tidal stripping can arbitrarily reduce the subhalo mass, but this should not change the original accreted galaxy mass.

lation in Pérez-González et al. (2008b) draws from a large number of different observations, and thus is a representative "average." The mass function choice in Conroy & Wechsler (2009) is interesting because the authors do not directly present a stellar MF measurement. Rather, they present a fitted stellar MF versus redshift that is fitted to both various observations of stellar masses and to the history of galaxy SFR versus mass and redshift. As such, the well-known discrepancy between high-redshift SFRs and stellar mass buildup is apparent (see Hopkins & Beacom 2006). The authors address this by adjusting the stellar MF at high redshifts to fit the SFR measurements. As such, it represents a completely independent constraint on the stellar MF evolution, and is representative of the stellar MF that would be obtained with fairly radically different assumptions (for example, a stellar IMF that evolves with redshift). To this extent, it provides something of an upper limit to the uncertainties in the galaxy mass-halo mass mapping.

Note that other methods of HOD fitting (other than our rank-ordering approach) yield very similar results. Allowing e.g. for scatter in the $M_{\rm gal}-M_{\rm halo}$ relation or fitting some prior assumed functional form (say e.g. a double-power law relation between these quantities, separately for central and satellite galaxies, with assumed lognormal scatter), yields little difference from the rank-ordering method and very small ($<0.1\,$dex) scatter (see e.g. Conroy & Wechsler 2009; Wang et al. 2006; Pérez-González et al. 2008a; Brown et al. 2008; Behroozi et al. 2010). We consider such methodological distinctions in § 6, and find that they make little difference to our conclusions.

2.2.2. *Attaching Other Galaxy Properties*

If and when other galaxy properties are required as input for the model, these too are assigned according to observations. For example, in § 5.4 we consider galaxy gas fractions. These are assigned to each galaxy according the observed correlations between galaxy gas mass and stellar mass, which have been quantified at a range of redshifts from $z=0-3$. As discussed there, we have compiled observations from the available sources, spanning this redshift range and a stellar mass range from $M_*\sim 10^{10}-10^{12}\,M_\odot$ (more than sufficient dynamic range for the predictions of interest here), specifically from Bell & de Jong (2000); McGaugh (2005); Calura et al. (2008); Shapley et al. (2005); Erb et al. (2006); Puech et al. (2008); Mannucci et al. (2009); Cresci et al. (2009); Forster Schreiber et al. (2009); Erb (2008); Mannucci et al. (2009).

We find that these observations can be well-approximated as a function of galaxy stellar mass and redshift with the fitting functions presented in Stewart et al. (2009b), and therefore simply adopt those, with a simple lognormal scatter term of $\sim 0.2\,$dex representative of the observed scatter at a given stellar mass. But adopting any individual measurement of these quantities instead gives very similar results.[11] Of course, the uncertainties in gas fractions and other properties increase at higher redshifts, but these are still sub-dominant in their ultimate effects compared to the growth in uncertainty in the stellar mass function itself.

2.3. *Step 3: Halo-Halo Mergers*

The next step towards identifying merging galaxies is to identify merging halos. The halo-halo merger rate (i.e. the rate at which formerly primary halos are accreted onto other primary halos and thus become subhalos) is well-measured in cosmological simulations and defined in the extended Press-Schechter formalism. In our default model, we determine this rate, as a function of halo mass, merging halo mass ratio, and redshift, from the fits presented in Fakhouri & Ma (2008b), determined from high-resolution N-body simulations (Springel et al. 2005c). We can include scatter in this as well; Fakhouri & Ma (2008a) quantify the scatter in halo-halo merger rates across populations. For a given halo population and arbitrary time interval, we can then statistically assign all halo-halo mergers that have occurred in that interval. We vary the determination of the halo-halo merger rate in § 6 (using e.g. the results of different dark matter simulations, simulations with gas included, and selecting halos differently), and find that it makes little difference.

The galaxy properties of the secondary are defined at the time when it first becomes a subhalo – i.e. when the secondary halo mass is its infall/maximum pre-accretion mass (when the halo-halo merger occurs). The primary galaxy continues to obey the normal $M_{\rm gal}-M_{\rm halo}$ relation for its total halo mass. So if the $M_{\rm gal}-M_{\rm halo}$ relation evolves with redshift, the primary galaxy will lie on the relation defined at the moment the actual merger occurs. The secondary will lie on the relation defined at the moment of the halo-halo merger (the subhalo instantaneous mass by the time of merger being much smaller). This is the basis for the rank-ordering method of assigning subhalo populations, and is key to the agreement between the observed small-scale clustering of galaxies and that produced by the models here.

2.4. *Step 4: From Halo-Halo to Galaxy-Galaxy Merger*

Of course, a halo-halo merger is not a galaxy-galaxy merger. We need to follow the recent subhalos until the time when the galaxies themselves will actually merge. There are two general methods to do this. The first, and our choice in this "default" model, is to assign a "merger time" – essentially, a delay timescale, usually calibrated from the results of high-resolution simulations, that represents the time for orbital decay from the initial halo-halo merger. This is the standard approach adopted in many semi-analytic models and models based on the extended Press-Schechter formalism. There are different possible choices for this merger time, and we will consider several of them in § 6. For our default model, we adopt the most common: the dynamical friction time. Specifically, we use the dynamical friction timescale for galaxy-galaxy merger with respect to the initial halo-halo

[11] At $z=0$, the gas fractions measured are based on measured atomic HI gas fractions; Bell & de Jong (2001) correct this to include both He and molecular H_2; McGaugh (2005) correct for He but not H_2; Kannappan (2004) gives just the atomic HI gas fractions (this leads to slightly lower estimates, but still within the range of uncertainty plotted; H_2 may account for $\sim 20-30\%$ of the dynamical mass, per the measurements in Jogee et al. 2005). We emphasize that these gas fractions are lower limits (based on observed HI flux in some annulus). At $z=2$, direct measurements are not available for most samples; the gas masses from Erb et al. (2006) are estimated indirectly based on the observed surface densities of star formation and assuming that the $z=0$ Kennicutt law holds. However other observations suggest that it does indeed hold (Bouché et al. 2007), and other indirect estimates yield similar results (Cresci et al. 2009; Mannucci et al. 2009). Moreover recent observations have been able to directly measure the molecular gas content of galaxies at $z\sim 2-4$, and where available these measurements agree very well with the assumed $f_{\rm gas}(M_*,z)$ relations used here (see e.g. Tacconi et al. 2010). We therefore conclude that although appropriate caution is due at high redshift, radical departures from our assumptions are unlikely.

merger, calibrated as a function of galaxy mass, mass ratio, redshift, and orbital parameters in high-resolution merger simulations in Boylan-Kolchin et al. (2008). Specifically the formula they present is:

$$t_{\rm df} = 0.0216\,H^{-1}\,\frac{(M_1/M_2)^{1.3}}{\ln(1+M_1/M_2)}\,\exp[1.9\,\eta]\left[\frac{r_c(E)}{r_{\rm vir}}\right] \quad (1)$$

where H is the Hubble constant at z, M_1 and M_2 the halo masses at the moment of the halo-halo merger, $\eta = j/j_c(E)$ is the standard "circularity parameter" ($\langle\eta\rangle \approx 0.5$), and $r_c(E)$ is the circular radius for an orbit with energy E (trivially related to the pericentric passage distance $r_{\rm peri}/r_{\rm vir}$, more usually quoted). Note that this explicitly depends on the merger orbital parameters. This allows us to incorporate the scatter in merger times seen in full cosmological simulations. Specifically, the cosmological distribution of the orbital parameters η and $r_{\rm peri}/r_{\rm vir}$ are presented in Benson (2005); Khochfar & Burkert (2006). Drawing randomly from these distributions, we can thus determine some Monte Carlo merger population.[12]

In general, varying the prescription for the merger "delay," across the entire physically plausible range, as we do in § 6, leads to factor ~ 2 systematic differences in the merger rate.

An alternative approach to following galaxies to their galaxy-galaxy merger from the halo-halo merger is to track the subhalos directly in cosmological simulations. In other words, given some cosmological population of halos, we can follow the bound substructure of the subhalo after an initial halo-halo merger, until the subhalo reaches some sufficiently small radius or is completely disrupted, at which point we define the "merger" to have occurred. Given this methodology, we can define a "subhalo" merger rate – i.e. a merger rate of subhalos being destroyed in primary halos (as opposed to a rate of those subhalos simply "falling into" those halos). If the simulation is sufficiently high resolution, the subhalo final merger/destruction should correspond closely to the actual galaxy-galaxy merger between the primary halo central galaxy and the satellite galaxy hosted by the subhalo (actually, so long as the subhalos are tracked long enough that the "remaining" merger time, after subhalo destruction, is small relative to the Hubble time, this is sufficient).

With such a measured subhalo destruction rate from simulations, we can convolve with the determined $M_{\rm gal} - M_{\rm halo}$ distribution and define directly the galaxy-galaxy merger rate. Again we stress that $M_{\rm halo}$ for the subhalos, as enters into this calculation and determines $M_{\rm gal}$ is the infall or maximum pre-accretion mass (as it generally should be, since the galaxy, pre-accretion, would lie on the $M_{\rm gal} - M_{\rm halo}$ relation for a normal central galaxy, not "knowing" it would be accreted at some time in the future), as the subhalo instantaneous (post-accretion, stripped) mass goes to zero at the time of destruction/merger. Such an approach automatically accounts for e.g. the orbit distribution of subhalos; however, it has its own uncertainties – subhalos are not baryonic galaxies, and the subhalo-subhalo merger time can differ from the galaxy-galaxy merger time by factors of up to several (owing to the resonant effects of baryons, and finite resolution limits). In any case, in § 6, we will consider several such determinations of the subhalo merger rates instead of our merger "delay" approach, with each using slightly different methodologies (see e.g. Stewart et al. 2009a; Kravtsov et al. 2004; Zentner et al. 2005; van den Bosch et al. 2005), and show that they yield similar results to our merger "delay" approach. We should note that the formula from Boylan-Kolchin et al. (2008) is calibrated as the total time from halo-halo merger to galaxy-galaxy merger in live simulations; thus, it implicitly includes all the effects seen in a full simulation (e.g. continuous mass loss/stripping of the satellites, resonant effects on near-passage of the galaxies, and baryonic effects on the halos).

Thus, after the convolution with the merger timescale, we obtain the rate of galaxy-galaxy mergers as a function of galaxy mass M_*, redshift z, and galaxy-galaxy baryonic mass ratio $\mu_{\rm gal}$.

2.5. *Step 5 (Optional): Linking Populations Across Different Epochs*

If we desire only instantaneous quantities (e.g. the merger rate), then what we have already described is entirely sufficient, and we can simply re-initialize the model at any redshift where we want to make predictions.

However, we will occasionally desire integral quantities (for example, how many mergers a given galaxy is likely to have experienced in its history). There are several choices of method to calculate these.

The simplest is our choice in the "default" model. Recall, we only need to integrate quantities such as the merger history *statistically*. And we will quote quantities such as the number of mergers for the primary branch of the halo merger tree. As such, we can use the fact that for a halo of mass M_0 at $z = 0$, the median primary progenitor mass at higher redshift $\langle M_h(M_0, z)\rangle$ (and its scatter) is a well-measured function from cosmological simulations (in other words, for a halo of mass M_0, we know the distribution of progenitor masses $M_h(M_0, z)$ at some higher z). We can then integrate over average histories, for example for the merger rate:

$$\langle N_{\rm merger}(M_0, \mu)\rangle = \int \frac{dN_{\rm merger}}{{\rm d}z}(M_h[M_0, z], z, \mu)\,{\rm d}z\,. \quad (2)$$

In our default model, we adopt the fits to the average halo growth tracks/progenitor mass distribution given as a function of halo mass and redshift in Neistein et al. (2006), calibrated to match the results of high-resolution N-body simulations. Of course, at each redshift z in the integral above, our steps $1-4$ are implicit in obtaining the relevant galaxy properties.

Note that this is effectively the same as beginning with some population of halos and evolving them forward along the average growth tracks defined by M_h above, where we integrate the halo mass forward using the merger rates and assign any shortfall to "unresolved" or "diffuse" accretion (since only mergers with mass ratios $\mu_{\rm gal} \gtrsim 10$ are of real significance here, it makes no difference if this mass technically comes from very small halos or truly diffuse material). This guarantees that the halo+subhalo population matches the total halo mass function at all times. Re-assigning quantities such as $M_{\rm gal}(M_{\rm halo})$ at each time, according to the observational constraints at each redshift, is equivalent to assigning the galaxy some net growth in stellar mass (star formation rate) and gas mass (inflow minus outflow), but without a prior on how much of each is in a bulge or disk component.[13] We

[12] Note that recently, Wetzel (2010) has shown that these distributions depend non-trivially on mass and redshift. However, the sense of that dependence is such that, if anything, the average merger timescales adopted here are always upper limits. As such, incorporating this more detailed dependence only strengthens our conclusions (see our discussion in § 6).

[13] If, for example via some rapid mergers, a galaxy exceeds the

can therefore compare the implied growth rate to observations, such as the observed stellar mass-star formation rate relation (Noeske et al. 2007a). For example, the interpolation between HODs at different redshifts implies that the SFR in star-forming galaxies scales very crudely as $\propto M_*^{(0.3-0.6)}\,(1+z)^{(1.5-2.5)}$ at $z \lesssim 2$ (with a sharp decline above the turnover mass $\sim L_*$), which agrees well with a number of different observational estimates (see e.g. Blain et al. 1999; Noeske et al. 2007b,a; Papovich et al. 2006; Martin et al. 2007; Bell et al. 2005; Damen et al. 2009). In fact, a more rigorous comparison shows quite good agreement – this exercise, for a halo occupation model that is effectively equivalent to the one used here, is presented in Conroy & Wechsler (2009), who find very good agreement both with observations of the integrated SFR versus redshift and the specific SFR in galaxies at different masses. Also, see Lee et al. (2009) and Zheng et al. (2007), who perform a corresponding analysis and obtain similar conclusions. The variation in predictions between our different models is comparable to that in the different models considered in these papers. (And recall, at least one of the mass function fits we adopt throughout is adjusted specifically to match the SFR versus galaxy mass and redshift relation; as such, agreement with these observations is ensured by construction). And despite its simplicity, our approach effectively guarantees a match to various other halo occupation statistics including stellar mass functions and the fraction of active/passive galaxies as a function of mass (Yang et al. 2005; Weinmann et al. 2006a,b; Gerke et al. 2007).

2.6. *Step 6 (Optional): The Effects of Mergers on Morphology*

Finally, we can couple the model to what is seen in high-resolution simulations of galaxy-galaxy mergers, to say what effects mergers will have on the galaxy morphologies.

In the model here, the galaxies are initially (at high redshift) disks; when a merger occurs, we use the model results from Hopkins et al. (2009b) to determine how much of the galaxy is converted from disk to bulge. The models used a suite of several hundred high-resolution hydrodynamic simulations, including star formation, black hole growth, and feedback from both to quantify the efficiency of bulge formation as a function of merger mass ratio,[14] orbital parameters, gas fraction, and other properties. The large suite of simulations spans the parameter space of interest, so there are good simulation analogues to the cosmologically anticipated mergers here, for which we can simply adopt the fits therein to model their bulge formation.

The details are presented in Hopkins et al. (2009b) – specifically they provide fitting functions (their Equations 7-10 & 27) that give the exact fraction of both the stellar and gaseous disks converted to bulge, as a function of merger mass ratio, gas fraction, and orbital parameters (all quantities that are determined in our model).[15] These scalings are all tested against the suite of simulations therein, and shown to provide accurate fits with < 0.3 dex scatter over the entire dynamic range of merger types of interest for this paper (see their Figure 16). In detail, the authors there define "bulge" as the stellar population that is dynamically supported by dispersion (as compared to "disk" stars supported by rotation, and all cold gas, hence star formation, which is part of the disk). They show that this agrees fairly well with decomposition of the observable stellar mass profile into an exponential disk and $r^{1/4}$-law bulge. But the bulges thus defined are generally "classical" bulges, by various observational definitions; as such, this is the "bulge mass" that we predict in this paper (pseudobulges, in any case, are believed to form primarily via disk instabilities, which we are not modeling here). We refer to that paper for the full equations, but in an approximate sense, in a merger of mass ratio μ, a fraction $\sim \mu$ of the primary stellar disk is violently relaxed and adds its low-density material to the bulge, and a fraction $\sim (1-f_{\rm gas})\,\mu$ of the gas loses its angular momentum and participates in a nuclear starburst, adding high-density starburst material to the bulge. The factor $(1-f_{\rm gas})$ represents the fact that the gas cannot be violently relaxed as stars are (because it is collisional); rather, it must lose angular momentum to the stars (which have a mass fraction in the disk $\propto 1-f_{\rm gas}$) – so in systems with increasing gas fractions, the efficiency of gas angular momentum loss decreases. This has very important consequences both for understanding what has now been seen in essentially all simulations of sufficiently high gas-fraction disks (both high-resolution and cosmological; see e.g. Springel & Hernquist 2005; Robertson et al. 2006; Cox et al. 2008; Robertson & Bullock 2008; Okamoto et al. 2005; Scannapieco et al. 2008; Governato et al. 2007, 2008), and for the global census of bulge and disk populations and survival of e.g. thin disks (Stewart et al. 2009b; Hopkins et al. 2009g). The true scalings are more detailed (see Hopkins et al. 2009b) but this represents the important physics.

In § 6, we discuss the consequences of using other, less accurate approximations to the behavior seen in full high-resolution simulations of galaxy mergers. We find that so long as the key scalings with mass ratio are at least qualitatively similar, our conclusions are unchanged.

2.7. *Summary*

$M_{\rm gal}(M_{\rm halo})$ relation, our model implicitly assumes its growth stalls until the halo "catches up"; if it falls below the relation, it experiences the necessary gas accretion and star formation for itself to catch up.

[14] It is important to use the "appropriate" mass ratio, for which the scalings presented in Hopkins et al. (2009b) are calibrated. In detail, the authors find that the most dynamically relevant mass ratio is not strictly the baryonic galaxy-galaxy ratio $\mu_{\rm gal}$ nor the halo-halo ratio $\mu_{\rm halo}$. Rather, the important quantity is the tightly bound material that survives stripping to strongly perturb the primary. Generally speaking, this is the baryonic plus tightly bound dark matter mass (the central dark matter mass, being tightly bound in the baryonic potential well, is robust to stripping in simulations; Quinn & Goodman 1986; Benson et al. 2004; Kazantzidis et al. 2008; Purcell et al. 2009). This can be reasonably approximated as the baryonic mass plus dark matter mass within a small radius of one NFW scale length ($r_s = r_{\rm vir}/c$, where $c \sim 10$ is the halo concentration; i.e. a few disk scale lengths). We find that around this range in radii, our results are not very sensitive to the precise definition, and in general, the baryonic mass ratio $\mu_{\rm gal}$ is a good proxy for the mass ratio calculated with this baryonic+tightly bound dark matter mass. However, in e.g. dark-matter dominated systems such as low-mass disks, the difference is important in particular for the absolute efficiency of bulge formation. Therefore, since this is what the simulation results are calibrated for, we adopt this mass ratio definition to calculate the dynamics in a given merger. However, this is not observable; we therefore present the predicted merger rates and their consequences in terms of an observable and easily-interpreted ratio $\mu_{\rm gal}$ (this also makes it possible to compare to other results in the literature). Again, the qualitative scalings are the same, but it is important to use the full information available in the model to calculate the merger dynamics. We include all mergers above a minimum mass ratio $\mu_{\rm gal} \sim 0.01$, although our results are not sensitive to this limit so long as it is small.

[15] The efficiency of bulge formation does depend on merger orbital parameters – namely the relative inclination angles of the merging disks — so we simply draw them at random assuming an isotropic distribution of inclinations (allowing some moderate inclination bias makes no difference).

Together, these simple assumptions are sufficient to define a "background" galaxy population. There are degeneracies in the model – however, we are not claiming that this is unique nor that it contains any physics other than the number and effects of mergers. For our purposes, the precise construction of the empirical model is not important – our results are unchanged so long as the same galaxy mass-halo mass relation and gas fraction distributions are reproduced as a function of galaxy mass and redshift. The importance of all the above is the following. **(1)** Observed galaxy stellar mass functions, the galaxy stellar mass and halo or subhalo mass relations, and the distributions of galaxy gas fractions as a function of stellar mass and redshift are all reproduced exactly as observed, at all redshifts $z = 0-4$ where observational constraints exist, *by construction* in the model. **(2)** Observed galaxy-galaxy clustering, both on large scales (the "two-halo" term, where it is primarily a function of halo mass) and small scales (the "one-halo" term, where it reflects subhalo/satellite halo occupation statistics), at those redshifts $z = 0-4$, are also reproduced *by construction*. Since this is built into the model explicitly, we do not show such a comparison, but Conroy et al. (2006), Wang et al. (2006), and Zheng et al. (2007) all show illustrations demonstrating that the simple methodology here yields (again by construction) excellent agreement with observed galaxy-galaxy correlation functions from scales of 50 kpc through 10 Mpc, at redshifts $z = 0$, 1, 2, 3 and 4, as a function of galaxy mass or luminosity, and galaxy color. **(3)** The only purpose of simulations ultimately, in this model, is (as in all halo occupation models) to provide a means of linking (statistically) galaxies at two different times. In other words, knowing the observed distribution of galaxy stellar masses and their separations, we use the dynamics which can be followed in the simulation to say which of these galaxies will merge in a given time interval (or again, some statistically approximation such as which fraction of the systems inside some distance). Likewise, we can ask where the systems that have such mergers "end up" in halo or stellar mass.

Together, this defines the suite of models adopted here. This is, by construction, a minimal model, and may leave out important details. However, in § 6, we systematically vary the model assumptions, and find that our conclusions are robust.

3. THE CONSEQUENCES: HOW HALO OCCUPATION STATISTICS CHANGE GALAXY-GALAXY MERGER RATES

Figure 1 illustrates how the combination of halo-halo merger rates and the observed halo occupation distribution determines galaxy-galaxy merger rates.

First, we show the halo occupation function itself (top left of Figure 1): for our purposes, this function is summarized in the most important quantity, the average galaxy baryonic mass hosted by a halo of a given mass $M_{\rm gal}(M_{\rm halo})$. If galaxy formation were efficient this would simply be $M_{\rm gal} = f_b M_{\rm halo}$, where f_b is the Universal baryon fraction, and galaxy-galaxy mergers would directly reflect halo-halo mergers. However, the relation between $M_{\rm gal}$ and $M_{\rm halo}$ is non-trivial.

We show several observational constraints on this quantity at redshift $z = 0$ (although we note that it is not redshift-independent, according to the observational constraints used for the HOD herein). First, the combination of the observed abundance and clustering of galaxies of a given mass have long been known to set tight constraints on $M_{\rm halo}(M_{\rm gal})$. We show a recent determination of these constraints, from clustering and abundance of local SDSS galaxies in Wang et al. (2006).[16] Second, we show the empirical "monotonic" or "rank ordering" results: it has been shown that good fits to halo occupation statistics (group counts, correlation functions as a function of galaxy mass and redshift, etc.) over a range of redshifts $z = 0-4$ are obtained by simply rank-ordering all galaxies and halos+subhalos in a given volume and assigning one to another in a monotonic one-to-one manner (see e.g. Conroy et al. 2006; Vale & Ostriker 2006). Here we plot the results of this exercise using the $z = 0$ stellar mass functions from Bell et al. (2003). Third, we compare this to independent estimates of the average $M_{\rm halo}(M_{\rm gal})$ from weak lensing studies in Mandelbaum et al. (2006). Other independent constraints give nearly identical results: these include halo mass estimates in low-mass systems from rotation curve fitting (see e.g. Persic & Salucci 1988; Persic et al. 1996; Borriello & Salucci 2001; Avila-Reese et al. 2008), or in high-mass systems from X-ray gas or group kinematics (Eke et al. 2004; Yang et al. 2005; Brough et al. 2006; van den Bosch et al. 2007).

Because it is the total baryonic mass, not just the stellar mass, that matters for e.g. defining the dynamics in a merger (a galaxy can be very massive and, in principle, contain little stellar mass), we will focus throughout this paper on that quantity ($M_{\rm gal}$ and $\mu_{\rm gal}$). However, Figure 1 is qualitatively identical if we use just the stellar mass M_* instead. In future work (in preparation), we will compare the consequences for the HOD, merger rates, and observable quantities such as the merger fraction resulting from different choices M_*, $M_{\rm gal}$, $M_{\rm halo}$ etc. in the definitions of merger mass ratio.

The second ingredient in predicting merger rates is the halo-halo merger rate determined from N-body simulations. Defined as the number of halo-halo mergers per primary halo, per logarithmic interval in mass ratio $\mu_{\rm halo} \equiv M_{\rm halo,\,2}/M_{\rm halo\,1}$, per unit redshift (or per Hubble time), the halo merger rate function can be approximated as (Fakhouri & Ma 2008b)

$$\frac{{\rm d}N_{\rm mergers}}{{\rm Halo\,d}\log\mu_{\rm halo}\,{\rm dz}} \approx F(M_{\rm halo})\,G(z)\,\mu_{\rm halo}^{-1}\,\exp\left\{\left(\frac{\mu_{\rm halo}}{0.1}\right)^{0.4}\right\}. \quad (3)$$

In these units, halo merger rates are nearly mass and redshift-independent: $F(M_{\rm halo}) \approx 0.03\,(M_{\rm halo}/1.2\times10^{12}M_\odot)^{0.08}$ and $G(z) \approx ({\rm d}\delta_c/{\rm dz})^{0.37}$ are weak functions of $M_{\rm halo}$ and z, respectively (in terms of mergers per unit *time*, this rate increases roughly as $(1+z)^2$). A number of other authors give alternative fits (see e.g. Stewart et al. 2009a; Genel et al. 2008), but the salient features are similar: weak redshift and halo mass dependence (in these units), power law-like behavior at low mass ratios with a slope of roughly $\mu_{\rm halo}^{-1}$ and an excess above this power-law extrapolation at high $\mu_{\rm halo}$.

The (fractional) contribution to halo growth from each interval is just $\mu_{\rm halo}$ times the merger rate; we plot this quantity in Figure 1 (top right) as we are ultimately interested in which mergers contribute to bulge growth. Because halo-halo merger rates go roughly as $dN_{\rm merger}/d\log\mu_{\rm halo} \propto \mu_{\rm halo}^{-1}$ (reflecting the shape of the halo mass function itself, and the nearly scale-free nature of CDM cosmologies), similar mass is contributed to the halo from each logarithmic interval in $\mu_{\rm halo}$.

Convolving the halo-halo merger rates with the HOD (i.e.

[16] These authors and others determine constraints in terms of galaxy stellar mass M_*; where necessary, we use our standard fit to observed gas fractions as a function of galaxy stellar mass and redshift (see § 2) to convert freely between baryonic ($M_{\rm gal}$) and stellar (M_*) galaxy masses at all redshifts.

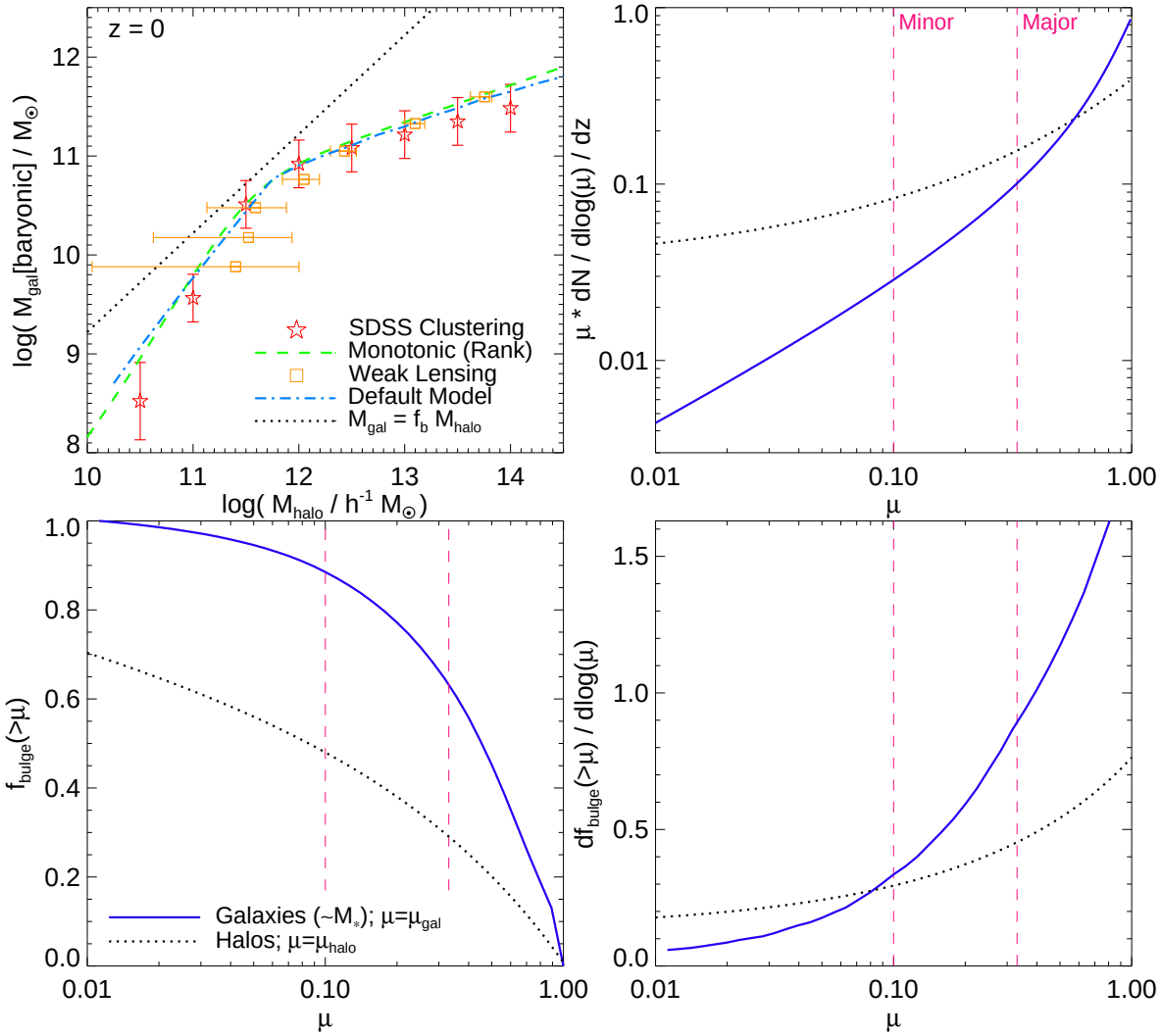

FIG. 1.— *Top Left:* Halo occupation: median baryonic galaxy mass of the primary galaxy in a halo or subhalo, as a function of that halo or subhalo's mass (at $z = 0$). For *central* galaxies, this refers to the total (primary) halo mass; for *satellite* galaxies, to their subhalo "infall" mass (i.e. mass the now-subhalo had at the last time it was a primary halo). Dotted line represents maximally efficient star formation (f_b is the Universal baryon fraction). We compare empirical constraints from clustering (Wang et al. 2006), weak lensing (Mandelbaum et al. 2006), and abundance matching ('monotonic'; Conroy et al. 2006). Our default model is constructed to match these constraints. *Top Right:* Differential contribution to growth from different mass ratio mergers, i.e. merger rate per logarithmic interval in mass ratio and unit redshift, $\mathrm{d}N_{\rm mergers}\,\mathrm{d}\log\mu^{-1}\,\mathrm{d}z^{-1}$, weighted by μ. Dotted line is for halos or, equivalently, would be for galaxies if $M_{\rm gal}\propto M_{\rm halo}$ were the actual HOD. Blue solid line is the result for $\sim L_*$ ($M_*\approx 10^{11}\,M_\odot$) galaxies, given the observed HOD. *Bottom Left:* Cumulative contribution of different mass ratio mergers to the $z = 0$ spheroid mass density (or halo mass density), integrated over all galaxy (halo) masses. *Bottom Right:* Differential version of the same. Because galaxy mass is not simply proportional to halo mass, bulge growth is dominated by major mergers while halo growth is contributed to by a wide range of mass ratios. We focus on $M_{\rm gal}$ rather than just the stellar mass M_* because the former, not the latter, matters for the dynamics in mergers; however the conclusions using M_* are qualitatively identical.

populating each halo with a galaxy of the appropriate mass), and the appropriate time lag between halo-halo and galaxy-galaxy merger, we obtain the galaxy-galaxy merger rate, now in terms of the *galaxy-galaxy* mass ratio $\mu_{\rm gal} = M_{\rm gal,\,2}/M_{\rm gal,\,1}$. In Figure 1, we compare this function (evaluated at $\sim L_*$ or $M_{\rm gal}\approx 10^{11}\,M_\odot$, where most of the stellar mass in the Universe is concentrated) to that obtained for halos.

Integrating over the galaxy history in our models, Figure 1 (bottom left) shows the fraction of the total $z = 0$ bulge/halo mass contributed by mergers with a mass ratio above some $\mu_{\rm gal}$, i.e.

$$f_{\rm bulge}(>\mu_{\rm gal}) \equiv \frac{1}{M_{\rm bulge}}\int \Theta(\mu'_{\rm gal}/\mu_{\rm gal})\,\mathrm{d}m_{\rm bulge}\ , \qquad (4)$$

where $\mu'_{\rm gal}$ refers to the mass ratio of the merger that formed each differential unit $\mathrm{d}m_{\rm bulge}$ of the final bulge mass $M_{\rm bulge}$, and $\Theta(x) = 1$ for $x > 1$ ($\mu'_{\rm gal} > \mu_{\rm gal}$) and $\Theta(x) = 0$ for $x < 1$ ($\mu'_{\rm gal} < \mu_{\rm gal}$). Note that this can be defined over the bulge mass of an individual galaxy, over all bulge mass in galaxies in a narrow interval in mass $M_{\rm gal}$, or over all galaxies (i.e. integrating over the bulge mass function). We show the latter.[17] We also show the differential version (bottom right): the fraction of $z = 0$ bulge mass contributed per logarithmic interval in merger mass ratio $\mathrm{d}f_{\rm bulge}/\mathrm{d}\log\mu_{\rm gal}$.

For halos (or equivalently for galaxies if the trivial mapping $M_{\rm gal}\propto M_{\rm halo}$ were true), the distribution of bulge mass fraction from mergers of different mass ratio is quite broad, as expected: only $\sim 50\%$ of halo mass comes from mergers

[17] In principle, some bulge mass could come from redshifts before our "initial" tracking of each halo, but in practice at any redshift, most of the mass has assembled relatively recently, so our results do not depend sensitively on the initial conditions.

with $\mu > 0.1$. Because halo-halo merger rates are nearly self-similar, the differential version of this reflects the instantaneous rate also shown, with similar contributions per logarithmic interval in halo mass ratio. It is still the case, though, that ten 1:10 mergers are less common than a 1:1 merger, meaning that major mergers dominate (Stewart et al. 2008).

In contrast, galaxy bulge assembly is biased much more towards high-mass ratio mergers, at least for $\sim L_*$ systems which dominate the mass density. This owes to the nature of halo occupation statistics: at low masses, galaxy mass grows rapidly with halo mass (galaxy formation is increasingly efficient as one moves from low masses closer to $\sim L_*$). Upon reaching $\sim L_*$, however, star formation shuts down relative to halo growth – in terms of the HOD, the scaling of galaxy mass with halo mass transitions from steep $M_{\rm gal} \propto M_{\rm halo}^{1.5-2.0}$ at low masses to shallow $M_{\rm gal} \propto M_{\rm halo}^{0.2-0.5}$ at high masses. In short, as halos grow in mass past $\sim 10^{12} M_\odot$, galaxy masses "pile up" near $\sim L_*$ ($M_{\rm gal} \sim 10^{11} M_\odot$), as can be seen in Figure 1. Since halo-halo merger rates are nearly self-similar in terms of halo-halo mass ratio, the "pileup" of galaxies near this mass means that a wide range of halo-halo mass ratios will be compressed into a narrow range of galaxy-galaxy mass ratios near $\mu_{\rm gal} \sim 1$ (see also Maller et al. 2006; Stewart et al. 2009a; Stewart 2009).

This is a general statement: in *any* scenario where $M_{\rm halo}/M_{\rm gal}$ has a minimum, the galaxy-galaxy merger rate will be weighted more towards major mergers than the halo-halo merger rate around (in particular at masses slightly above) that minimum. The minimum in $M_{\rm halo}/M_{\rm gal}$ is empirically well-established, and occurs near $\sim L_*$, where most of the mass density lies. It is therefore inevitable that the contribution to the integrated bulge mass will be more weighted towards major mergers than to the halo mass.

This is also easily understandable in terms of the mass functions of galaxies and halos. The halo mass function does not feature a sharp break, so the mass density of halos is broadly distributed over several orders of magnitude in halo mass. In contrast, the galaxy mass function reflects inefficient star formation at low and high masses, with a sharp break, and so the galaxy mass density is concentrated in a narrow range (a factor ~ 3) around the break L_*. The mass of subunits (which broadly reflects the global mass function) in halos therefore includes contributions from a wide range of mass ratios. In contrast, the bulge growth of a galaxy is dominated by systems near $\sim L_*$. At masses $\lesssim$ a few L_*, this means major mergers will be most important. It is not until an $\sim L_*$ galaxy represents a minor merger (i.e. galaxy masses $\gtrsim 3 L_*$) that minor mergers (again, mergers of those $\sim L_*$ galaxies) begin to dominate the mass assembly.

4. GALAXY-GALAXY MERGER RATES

4.1. *Scaling with Mass and Redshift*

We first examine the galaxy-galaxy merger rate, given these empirical constraints. Figure 2 shows the number of mergers, as a function of mass ratio, that a typical galaxy of a given $z = 0$ stellar mass has experienced since $z = 2$. We emphasize that this is for a sample mass-selected based on their $z = 0$ masses; a sample selected at the same mass at higher redshift will have a systematically larger number of mergers in a similar time or Δz interval (and will be higher mass by $z = 0$). Below, we discuss how these predictions compare with observations; the two generally agree well. We compare with the number of halo-halo mergers as a function of

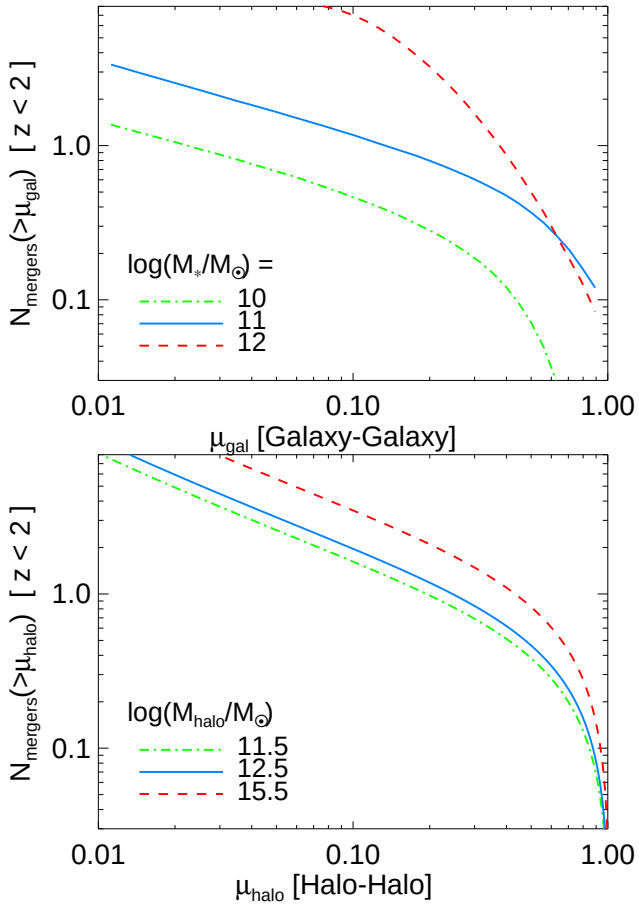

FIG. 2.— *Top:* Median number of galaxy-galaxy mergers since $z = 2$ above a given baryonic mass ratio $\mu_{\rm gal}$ for a $z = 0$ galaxy of the given stellar mass. The same mass selection at higher redshift intervals will systematically increase the number of mergers. The predictions here agree well with observational estimates (de Ravel et al. 2009; Conselice et al. 2009; Lin et al. 2008). *Bottom:* Same, for halo-halo mergers. Owing to the shape of the HOD, the merger rate is a steep function of galaxy mass around $\sim L_*$, whereas the halo-halo merger rate is only weakly mass-dependent. Galaxies near $\sim L_*$ have had ~ 1 major merger since $z = 2$.

halo mass ratio, for typical corresponding halo masses. The two are quite different, for the reasons discussed in § 3: essentially, at low masses, $M_{\rm gal} \propto M_{\rm halo}^2$, so a 1:3 $\mu_{\rm halo}$ merger becomes a 1:9 $\mu_{\rm gal}$ merger, and merger rates at each $\mu_{\rm gal}$ are suppressed. At high masses, $M_{\rm gal} \propto M_{\rm halo}^{0.5}$, and rates are correspondingly enhanced. At $\sim 10^{11} M_\odot$, where most of the spheroid mass density of the Universe resides, the typical galaxy has experienced $\sim 0.5-0.7$ major ($\mu_{\rm gal} > 1/3$) mergers since $z = 2$, a fraction that corresponds well to the observed fraction of bulge-dominated early-type systems at these masses (see e.g. Bell et al. 2003). At most masses (excepting the highest masses, where the shape of the HOD yields a strong preference towards minor mergers), the total number of mergers with $\mu_{\rm gal} \gtrsim 1/10$ is a factor $\sim 2-3$ larger than the number with $\mu_{\rm gal} > 1/3$, and at low mass ratios $\mu_{\rm gal} \ll 1/10$, the merger rate asymptotes to a power-law with $N(>\mu_{\rm gal}) \propto \mu_{\rm gal}^{-(0.25-0.5)}$.

Figure 3 shows how the median merger rates evolve with redshift, for four different intervals in mass. We compare the rate of major ($\mu_{\rm gal} > 1/3$) and major+minor ($\mu_{\rm gal} > 1/10$) mergers. We also compare different constraints on the HOD, from fitting different galaxy mass functions and clustering data. Specifically, we show the default model here, where

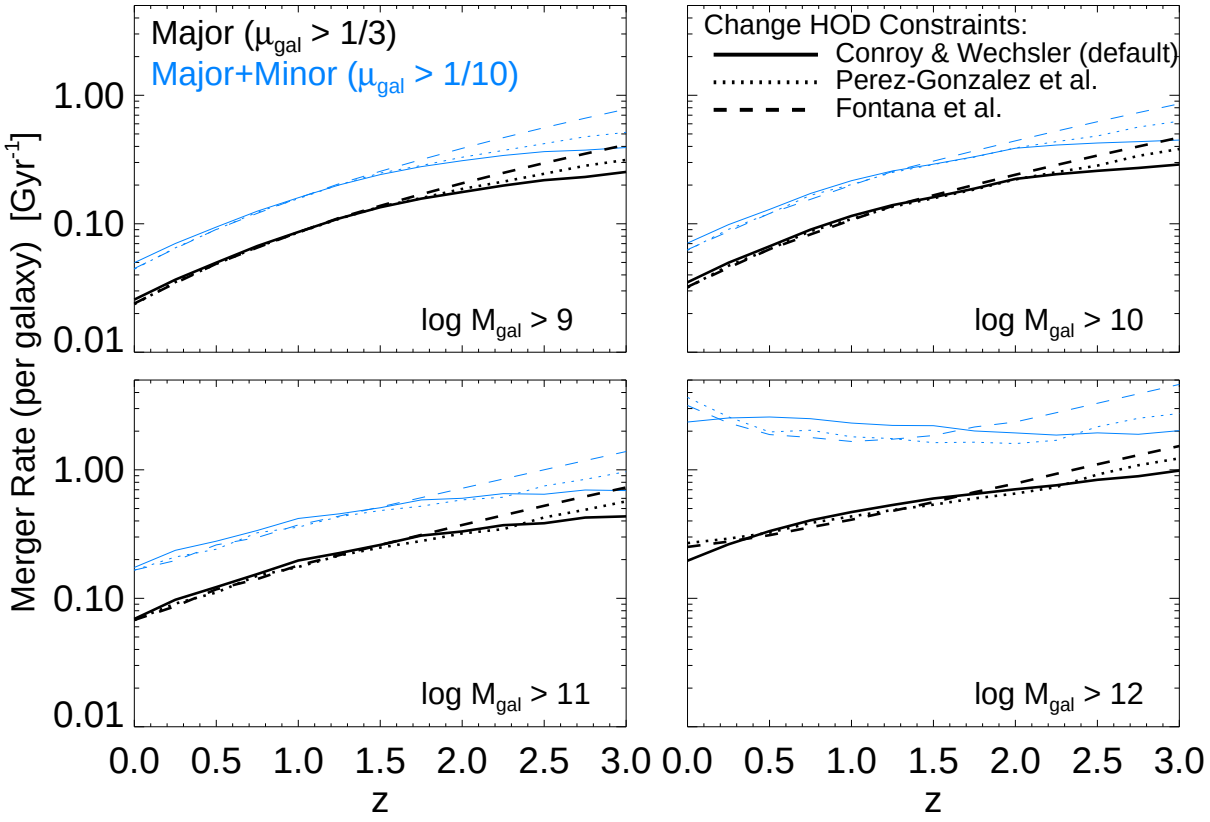

FIG. 3.— Merger rate (number of mergers per galaxy per Gyr) as a function of redshift for different galaxy mass intervals (all $M_{\rm gal}$ above some minimum baryonic mass in $M_\odot$ at each redshift). Solid, dashed, and dot-dashed lines correspond to three different halo occupation model constraints: uncertainties are small at $z < 2$. Colors correspond to the range of merger mass ratios.

the function $M_{\rm gal}(M_{\rm halo})$ is determined from fits to observed clustering, stellar mass functions, and star formation rate distributions in Conroy & Wechsler (2009); we compare the results adopting a monotonic ranking between galaxy and halo mass and using the redshift-dependent stellar mass functions from Fontana et al. (2006) or Pérez-González et al. (2008b). Further variations are discussed in detail in § 6. These illustrate the robustness of the model: empirical halo occupation constraints are sufficiently tight that they contribute little ambiguity in the resulting merger rate at $z < 2$. Above $z = 2$, the results begin to diverge, as the stellar mass function is less well-determined (and few clustering measurements are available); however these higher redshifts have relatively little impact on the predictions at low-z. The major merger rate increases with mass with a slope of roughly $\propto (1+z)^{1.5-2.0}$, but this is mass-dependent. The evolution in the galaxy-galaxy merger rate is somewhat shallower than the redshift evolution of the halo-halo merger rate (which scales with the Hubble time) as a consequence of the redshift evolution of the HOD.

4.2. *Comparison with Observations*

In Figure 4, we compare these predictions to observed major merger fractions. As most measurements of the merger fraction do not have a well-defined mass selection, we first simply consider a large compilation of observational results compared to the predicted merger rate of $\sim L_*$ galaxies. For now, because we are considering a range of mass and observational methodologies, we simply convert the predicted merger rate to an observed merger fraction assuming a constant observable lifetime $t_{\rm obs}$, here showing $t_{\rm obs} = 0.5\,$Gyr and $t_{\rm obs} = 1\,$Gyr, typical values in the literature. We also compare the number density of mergers versus mass, at a given redshift. The agreement appears reasonable, but there is a large scatter in the observations, mostly owing to different selection and merger identification criteria.

We can also compare the predicted integrated number of mergers in Figure 2 to various observational estimates. For

TABLE 1
OBSERVED MERGER RATES

Reference	Selection[1]	Symbol[2]
	Pairs	
Kartaltepe et al. (2007)	$20\,h^{-1}\,$kpc	blue triangles
Lin et al. (2004, 2008)	$30\,h^{-1}\,$kpc	pink circles
Xu et al. (2004)	$20\,h^{-1}\,$kpc	blue circle
De Propris et al. (2005)	$20\,h^{-1}\,$kpc	black asterisk
Bluck et al. (2009)	$20\,h^{-1}\,$kpc	orange squares
Bundy et al. (2009)	$20\,h^{-1}\,$kpc	green stars
Bell et al. (2006b,a)	$20\,h^{-1}\,$kpc	red pentagons
	Morphology	
Conselice et al. (2009)	CAS	pink ×'s
Conselice et al. (2008)	CAS	blue ×'s
Cassata et al. (2005)	CAS	cyan inverted triangles
Jogee et al. (2008)	visual	pink triangles
Bundy et al. (2005)	visual	light green stars
Wolf et al. (2005)	visual	orange diamonds
Bridge et al. (2007, 2010)	visual	purple squares
Lotz et al. (2006, 2008b)	Gini-M20	dark green +'s

[1] Selection criterion used to identify merger candidates. For pair samples, this refers to the pair separation. For morphological samples, to the method used.
[2] Symbol used for each sample in Figures 4 & 5.

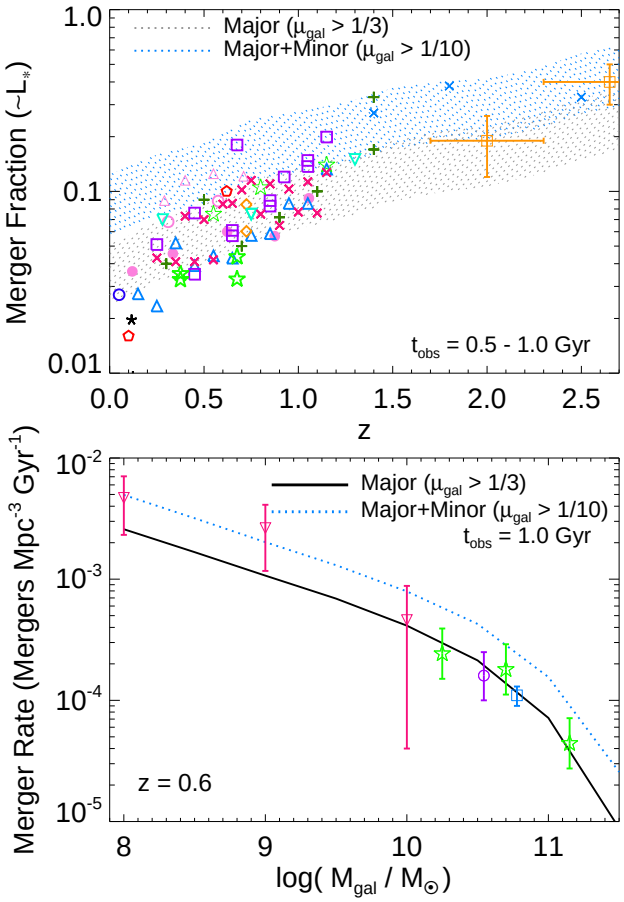

FIG. 4.— *Top:* Major merger fraction of $\sim L_*$ galaxies. Observations (with the symbol type for each) are listed in Table 1; for now, we treat them all the same. Shaded range corresponds to the predicted merger rate, convolved with an observable lifetime $t_{\rm obs} = 0.5-1.0\,$Gyr (color denoted the mass ratio range, as labeled). *Bottom:* Integrated merger rate as a function of galaxy mass at $z = 0.6$ (in absolute units, mergers per Mpc^3 per Gyr above some minimum mass), where observations span the greatest dynamic range. Observations are from Bell et al. (2006a, blue square), Conselice et al. (2009, pink triangles), Bundy et al. (2009, green stars), and López-Sanjuan et al. (2009b, purple circle). Here, morphological samples are converted to rates with $t_{\rm obs} = 1\,$Gyr; pair samples the appropriate timescales for their separation (see text). Predicted rates agree with those observed, but there is considerable scatter between various observational selection methods.

example, de Ravel et al. (2009) use pair-selected samples to estimate that $\sim 20-25\%$ of the $M_* > 10^{10}\,M_\odot$ population has experienced a merger with mass ratio $\mu > 0.25$ since $z = 1$; Conselice et al. (2009) estimate a similar number of mergers for $M_* > 10^{10}\,M_\odot$ galaxies since $z = 1$ and about again as many since $z = 2$, they also find that the number of mergers increases significantly with galaxy mass; Lin et al. (2008) estimate that $\sim 54\%$ of L_* ($M_* \sim 10^{11}\,M_\odot$) galaxies have experienced a $\mu > 0.25$ merger since $z = 1.2$. All of these predictions can be compared with our predictions in Figure 2, and they agree well (especially given different methodologies, masses, and redshift ranges involved).

In order to test more strictly, and to take advantage of where observable merger timescales have been rigorously calibrated, in Figure 5 we restrict our comparison to galaxy-galaxy mergers identified observationally using a consistent methodology and covering a well-defined mass range.

First, we consider pair fractions: specifically the fraction of *major* ($\mu_{\rm gal} > 1/3$) pairs with small projected separations $r_p < 20\,h^{-1}\,$kpc (often with the additional requirement of a line-of-sight velocity separation $< 500\,{\rm km\,s^{-1}}$), and stellar masses $M_* \sim 1-3\times10^{10}\,M_\odot$ or $M_* \sim 0.5-2\times10^{11}\,M_\odot$. For each mass bin, the pair fractions as a function of redshift can be empirically converted to a merger rate using the merger timescales at each radius. Lotz et al. (2008a, 2009b,a) specifically calibrate these timescales for the same projected separation and velocity selection from a detailed study of a large suite of hydrodynamic merger simulations (including a range of galaxy masses, orbital parameters, gas fractions and star formation rates) using mock images obtained by applying realistic radiative transfer models, with the identical observational criteria to classify mock observations of the galaxies at all times and sightlines during their evolution. For this specific pair selection criterion (if we average over the typical distribution of mass ratios for mergers selected in this interval), they find a median merger timescale of $t_{\rm merger} \approx 0.35\,$Gyr, with relatively small scatter and very little dependence on simulation parameters ($\pm 0.15\,$Gyr).[18] We use their median $t_{\rm merger}$ to convert the observations to a merger rate. Because of the weighting over merger mass ratio and orbital parameters, for which the explicit dependence is presented in these papers, we obtain the same result (within the observational error bars) if we convolve our predicted merger rates with the explicit observable merger timescale as a function of merger gas fraction, galaxy mass, redshift, mass ratio, and orbital parameters, as presented in Lotz et al. (2009b,a). Completeness corrections are discussed in the various papers; we also adopt the standard correction from Patton & Atfield (2008), calibrated to high-resolution simulations, for the fraction of systems on early or non-merging passages (to prevent double-counting systems on multiple passages); but this is relatively small ($20-40\%$; see also Lotz et al. 2008a).

The advantages of these pair fractions are that: (1) the mass ratio can be determined, leading to little contamination from minor mergers,[19] (2) at such small separations, most such pairs will eventually merge, and (3) there is little ambiguity in the merger timescale, with only a factor $\sim 10-20\%$ systematic uncertainty in the median/average merger timescale in high-resolution calibrations (with a $\sim 25-50\%$ dispersion or variation always present about that median, owing to cosmological variation in e.g. the exact orbital parameters).

Second, we consider morphologically-selected mergers, identified on the basis of by-eye classification or automated morphological criteria such as the concentration-asymmetry (CAS) or Gini-M20 planes (see e.g. Conselice et al. 2003; Lotz et al. 2004). Lotz et al. (2008a) also attempt to calibrate

[18] The merger timescale from simulations at this radius is shorter than the time obtained assuming dynamical friction and circular orbits in e.g. an isothermal sphere, as has commonly been done (this is assumed in e.g. both Patton et al. 2002; Kitzbichler & White 2008). This owes to two effects: first, angular momentum loss at these radii is *not* dominated by dynamical friction, but rather by exchange in strong resonances that act much more efficiently (even allowing for e.g. mass loss by the secondary inside the primary halo, which is of course included in the high-resolution simulations, this has the net effect of significantly accelerating most mergers). Second, by these radii, even initially circular orbits have become highly radial, leading to shorter merger times. Because of these effects, the remaining merger time at this scale depends only weakly on initial conditions or orbital parameters – essentially, these processes have erased most of the "memory" of the original orbital configuration. This emphasizes the importance of using full simulations with baryonic effects in calibrating these timescales.

[19] Note that many older studies adopt the galaxy-galaxy luminosity ratio as a proxy for mass ratio. This is not a bad approximation in e.g. numerical simulations, but could be subject to bias from e.g. differential enhancement in star formation. Obviously it is preferable to use an actual stellar mass ratio where possible. Restricting our samples to just studies with stellar masses, however, we obtain similar conclusions.

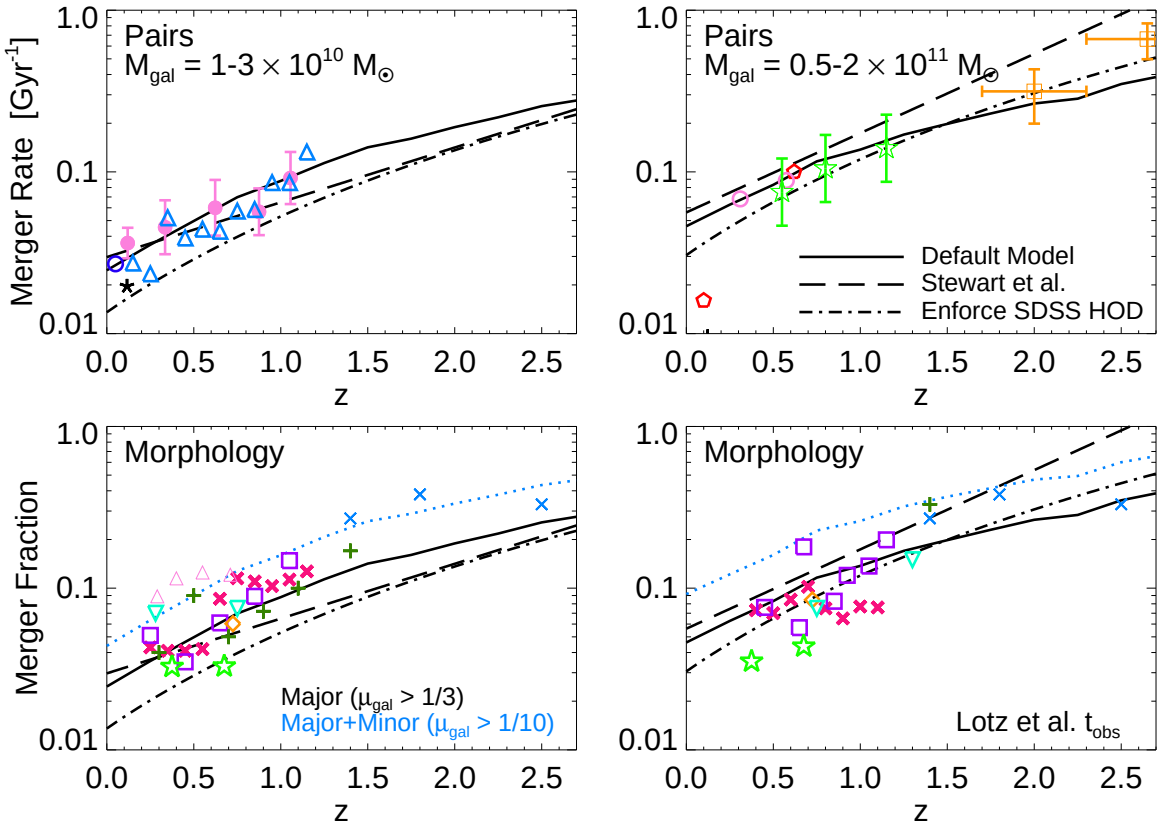

FIG. 5.— *Top:* Predicted merger rate in different stellar mass intervals, compared to that inferred from close pair studies (projected $r < 20\,h^{-1}$ kpc). Observations (with point types) are listed in Table 1; they are converted to merger rates given the calibration of merger times as a function of pair separation from high-resolution N-body simulations in Lotz et al. (2008a, 2009b,a). We show our default model, as well as the "instantaneous" calculation obtained by assuming all galaxies lie on the $z = 0$ (non-evolving) SDSS HOD shown in Figure 1. We also show the results from Stewart et al. (2009a), using different simulation merger rates, merger trees, and HOD constraints. *Bottom:* Morphologically identified merger fraction in the same mass intervals, compared with predictions. The assumed timescale for identification as morphologically disturbed is ~ 1 Gyr, again calibrated from simulations in Lotz et al. (2008a). Observations in this case could be contaminated by minor mergers; we therefore show both major and major+minor merger fractions. The scatter is larger in morphological samples (with some probably contamination), but predictions agree within a factor ~ 2.

the observable timescale for classification of major mergers via the Gini-M20 criterion, at rest-frame wavelengths and masses of the observations. They find an observable timescale $t_{\rm obs}(\rm Gini-M20) \sim 1$ Gyr, and we adopt that here, but note that the predicted timescale in this case depends much more sensitively on the depth of the observations, the waveband adopted, and properties such as the gas-richness of the merging systems.[20] Moreover, although, by definition, this methodology is complete to events that have violently disturbed the galaxy, the level of disturbance at a given merger mass ratio depends on orbital parameters and galaxy gas fractions, so a fixed level of disturbance does not correspond to a fixed merger mass ratio. Some contamination from minor mergers is likely. Jogee et al. (2009) estimate empirically that $\sim 30-40\%$ of their (by-eye) morphologically-identified sample represent contamination from $1/10 < \mu_{\rm gal} < 1/3$ minor mergers. We therefore compare the predicted merger fraction for $\mu_{\rm gal} > 1/3$ and $\mu_{\rm gal} > 1/10$. Allowing for this range, the observations agree well with the predictions. In particular, the observations using a calibration of Gini-M20 or CAS specifically matched to high-resolution hydrodynamic major merger simulations (e.g. Lotz et al. 2008b; Conselice et al. 2009) agree reasonably well with the predicted $\mu_{\rm gal} > 1/3$ fractions. And external, purely empirical indicators favor similar merger timescales (see e.g. Conselice 2009).

A quantity closely related to the pair fraction on small scales is the galaxy-galaxy autocorrelation function (specifically that on small scales, inside the "one halo term" where it reflects galaxies inside the same parent halo). Effectively this generalizes the predicted pair fraction from $< 20\,h^{-1}$ kpc to all scales. But recall, the adopted halo occupation-based methodology is designed, by construction, to match the observed correlation functions as a function of mass. It is therefore guaranteed that the clustering at scales ~ 100 kpc through $\gtrsim 10$ Mpc is reproduced as a function of galaxy mass and redshift (for explicit illustrations, see e.g. Conroy et al. 2006; Zheng et al. 2007; Wang et al. 2006).

4.3. *Analytic Fits*

It is useful to quantify the predicted merger rates with simple analytic fitting functions.

First, consider major mergers. We find that the major merger rate (number of $\mu_{\rm gal} > 1/3$ mergers per galaxy per

[20] For the explicit dependence on these parameters, see Lotz et al. (2009b,a). Note that the timescale of 1 Gyr here is slightly longer than the 0.6 Gyr estimated directly from observations in Conselice (2009) (although within their quoted 1σ error bars) and in the original Lotz et al. (2008a) for radial 1:1 mergers. The difference in the latter owes to the dependence of observable timescale on gas fraction as calibrated in Lotz et al. (2009a) (here we adopt a median appropriate for the median gas fractions of the model galaxies), and from the dependence on merger mass ratio as calibrated in Lotz et al. (2009b) (where our value here represents a weighting over the mass ratio distribution down to mass ratio $\mu = 1/3$ as appropriate for the observations here). In any case, the difference is generally smaller than the scatter between different observational estimates.

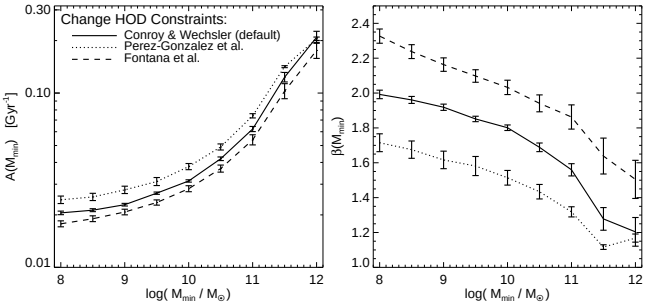

FIG. 6.— Results of fitting the major merger rate as a function of mass and redshift to a function of the form of Equation 5. Linestyles correspond to different HOD choices, as in Figures 3-5. *Left:* Normalization, i.e. number of mergers per galaxy per Gyr at $z = 0$, for galaxies above a minimum mass $M_{\rm min}$. *Right:* Redshift dependence, i.e. slope β given a merger rate per unit time $\propto (1+z)^{\beta}$, as a function of minimum mass. The mass-dependent $A(M_{\rm min})$ and β can be approximated with Equations 6-7, with systematic uncertainties of 0.3 dex and 0.2, respectively.

unit time), for galaxies above a given minimum stellar mass threshold ($M_* > M_{\rm min}$), can be well-fitted by the following simple function:

$$\frac{{\rm d}N_{\rm major}}{{\rm d}t} = A(M_{\rm min})\,(1+z)^{\beta(M_{\rm min})}\ \ [\text{per galaxy}], \qquad (5)$$

i.e. a $z = 0$ normalization $A(M_{\rm min})$ and simple power-law scaling with redshift with slope $\beta(M_{\rm min})$. Figure 6 shows these quantities, fitted to the predictions shown in Figures 3-5, as a function of the mass $M_{\rm min}$. The trends discussed above are evident: the normalization of merger rates increases with mass, and (albeit more weakly), the dependence on redshift decreases with mass. This normalization and redshift variation can be approximated with the scalings:

$$A(M_{\rm min})_{\rm major} \approx 0.02\left[1+\left(\frac{M_{\rm min}}{M_0}\right)^{0.5}\right]\,{\rm Gyr}^{-1} \qquad (6)$$

and

$$\beta(M_{\rm min})_{\rm major} \approx 1.65 - 0.15\log\left(\frac{M_{\rm min}}{M_0}\right). \qquad (7)$$

where $M_0 \equiv 2\times10^{10}\,M_\odot$ is fixed. There is a systematic factor ~ 2 uncertainty in the merger rate normalization $A(M_{\rm min})$ at all $M_{\rm min}$, considering the range of models discussed in detail in § 6 below. The uncertainty in $\beta(M_{\rm min})$ is illustrated in Figure 6, approximately a systematic $\Delta\beta \sim 0.15-0.20$.

These fits are for major ($\mu_{\rm gal} > 1/3$) mergers. To rough approximation, the number of mergers as a function of mass ratio scales with the approximate form

$$\frac{{\rm d}N(>\mu_{\rm gal})}{{\rm d}t} \propto \mu_{\rm gal}^{-0.3}\,(1-\mu_{\rm gal})\ \ [\text{per galaxy}] \qquad (8)$$

(derived and discussed in more detail in Stewart et al. 2009a). This is a good approximation as long as the galaxy is within an order of magnitude of $\sim L_*$. For the range where this function is a good approximation, it implies an approximately constant ratio of a factor ≈ 2 ($0.3-0.4$ dex) of major+minor ($\mu_{\rm gal} > 1/10$) to major ($\mu_{\rm gal} > 1/3$) mergers.

More specifically, we can fit a function of the form of Equation 5 to the major+minor ($\mu_{\rm gal} > 1/10$) merger rate of galaxies above some $M_{\rm min}$, and obtain the best-fit scalings

$$A(M_{\rm min})_{\rm minor} \approx 0.04\left[1+\left(\frac{M_{\rm min}}{M_0}\right)^{0.8}\right]\,{\rm Gyr}^{-1} \qquad (9)$$

and

$$\beta(M_{\rm min})_{\rm minor} \approx 1.50 - 0.25\log\left(\frac{M_{\rm min}}{M_0}\right), \qquad (10)$$

with similar systematic uncertainties in both $A(M_{\rm min})$ and $\beta(M_{\rm min})$ to the major merger rate. Note that these equations should be treated with caution for the most massive systems – the simple fitting functions do not extrapolate to arbitrarily high mass and the direct numerical results (e.g. Figure 3) should be used.

5. THE RELATIVE CONTRIBUTIONS TO BULGE GROWTH FROM DIFFERENT MERGERS

5.1. *Overview*

Figure 7 illustrates how the efficiency of bulge formation scales in simulations. We show how the average B/T resulting from disk-disk mergers scales with mass ratio (approximately $\mu_{\rm gal}$, but see § 2), gas fraction $f_{\rm gas}$, and merger orbital parameters, according to the fits to the hydrodynamic simulations in Hopkins et al. (2009b). To lowest order, as discussed in § 3, the amount of bulge formed (the amount of stellar disk of the primary galaxy that is violently relaxed, and amount of gas disk that is drained of angular momentum and participates in the nuclear starburst) scales linearly[21] with the mass ratio of the encounter, $\propto \mu_{\rm gal}$. This conclusion – ultimately the important statement for our analysis – has been reached by numerous independent simulation studies, adopting different methodologies and numerical techniques, and naturally follows from the simple gravitational dynamics involved in violent relaxation (see e.g. Hernquist 1989; Barnes & Hernquist 1992; Mihos & Hernquist 1994b, 1996; Naab & Burkert 2003; Bournaud et al. 2005; Younger et al. 2008a; di Matteo et al. 2007; Hopkins et al. 2009b; Cox et al. 2008). In addition, observational constraints on the efficiency of merger-induced star formation support these estimates (Woods et al. 2006; Barton et al. 2007; Woods & Geller 2007).

At fixed mass ratio, the bulge formed (remnant B/T) can vary considerably depending on orbital parameters of the merger, in particular the relative inclinations of the disks (prograde or retrograde). This variation is shown in Figure 7. However, in a cosmological ensemble, this will average out. Here, we assume random inclinations, but allowing for some preferred inclinations amounts to a systematic offset in the B/T predicted and will not change our conclusions regarding the relative importance of different mass ratios for bulge formation.

Another important parameter determining B/T is the merger gas fraction. To lowest order, angular momentum loss in gas is suppressed by a factor $\sim (1-f_{\rm gas})$; as a result, the efficiency of bulge formation (B/T expected for a merger of a given mass ratio) is suppressed by the same factor. This can have dramatic cosmological implications, because $f_{\rm gas}$ is a strong function of galaxy mass; these are discussed in detail in Hopkins et al. (2009g). Figure 7 shows the observed dependence of disk/star-forming galaxy gas fractions on stellar mass at $z = 0$ and $z = 2$; if we assume mock galaxies on the $z = 2$ relation each undergo a merger of a given mass ra-

[21] Note that this refers to the mass fraction which is violently relaxed, thus adding to the bulge. Disk heating and resonant processes that contribute to the thick disk or disk substructure are different. For example, Hopkins et al. (2008e) show that disk heating in minor mergers is second-order in mass ratio; Purcell et al. (2009) and Kazantzidis et al. (2009) reach similar conclusions (albeit with slightly different absolute normalization/efficiency).

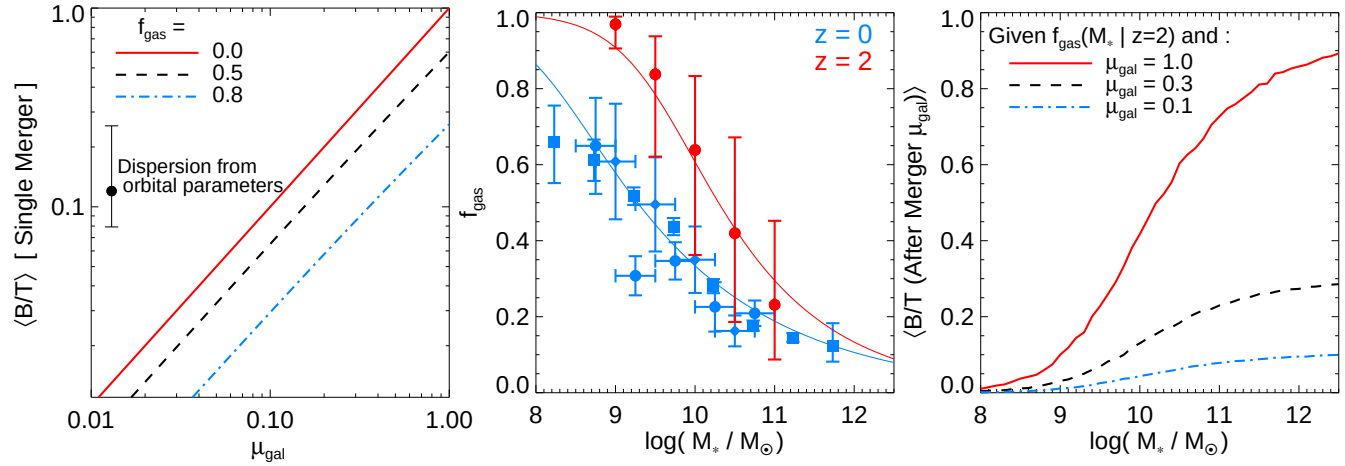

FIG. 7.— *Left:* Average bulge-to-total ratio B/T (of the *classical* bulge) resulting from a single merger of mass ratio $\sim \mu_{\rm gal}$ between galaxies with gas fraction $f_{\rm gas}$ (from simulations in Hopkins et al. 2009b). To lowest order B/T scales as $\propto \mu_{\rm gal}\,(1-f_{\rm gas})$. Error bar shows scatter owing to the cosmological range of orbital parameters. *Center:* Median observed gas fraction and scatter (error bars) for disks of a given stellar mass at $z=0$ (blue) from Bell & de Jong (2001, diamonds), Kannappan (2004, squares), and McGaugh (2005, circles), and at $z=2$ (red) from Erb et al. (2006). Solid lines show fits to the median at each redshift. *Right:* Corresponding median B/T expected from mergers at $z=2$ with primary of a given stellar mass and mass ratio $\mu_{\rm gal}$ (given the observed $\langle f_{\rm gas}[M_*\,|\,z=2]\rangle$). Suppression of bulge formation by gas-richness is important for the absolute bulge mass formed (especially at low masses), but because it is $\mu_{\rm gal}$-independent, does not affect the relative contribution of major/minor mergers.

tio, then the resulting B/T at each mass is shown. Bulge formation will be significantly suppressed by high gas fractions in low-mass galaxies, giving rise to e.g. a strong mass-morphology relation similar to that observed (Stewart et al. 2009b; Hopkins et al. 2009g). However, it is clear in Figure 7 that the effect of $f_{\rm gas}$ is a systematic offset in B/T, independent of mass ratio. Because in what follows we will generally examine the *relative* importance of mergers of different mass ratios (independent of gas fraction), the inclusion or exclusion of the effects of gas on merger dynamics makes little difference to our conclusions.

Given these constraints from simulations on the amount of bulge formed in a given merger, and the merger rates predicted in § 4, Figure 8 shows the contribution of mergers of different mass ratios to the $z=0$ stellar mass in bulges (as Figure 1). We show this for galaxies in a narrow range of *total* stellar mass around three different values, and for the entire galaxy population (integrated over bulges of all masses). We specifically define this as the fraction of bulge mass formed or assembled in mergers that were above a given galaxy-galaxy mass ratio $\mu_{\rm gal}$. Considering different variations to the empirical and simulation constraints (see § 6), about $60-70\%$ of the globally integrated bulge mass is assembled by major mergers $\mu_{\rm gal}>0.3$, with another $\sim 30\%$ assembled by minor mergers $0.1<\mu_{\rm gal}<0.3$, and the remaining $\sim 0-10\%$ from a wide range of mass ratios $\mu_{\rm gal}\sim 0.01-0.1$.

Note that, for massive galaxies ($\gtrsim$a few L_*), where "dry" mergers become an important channel (assembling mass already in massive bulges), there is an ambiguity in the fraction $f_{\rm bulge}(>\mu_{\rm gal})$ "contributed" by mergers above a given $\mu_{\rm gal}$. Figure 8 illustrates this. We therefore introduce the distinction between bulge *formation* and bulge *assembly*, terms we will use throughout.

First, formation: we can define $f_{\rm bulge}(>\mu_{\rm gal})$ as the fraction of bulge mass originally *formed*, i.e. initially converted into bulge mass from disk mass (gas or stars) by mergers with some mass ratio $\mu_{\rm gal}$. In other words, taking Equation 4, where for each parcel of mass in the final bulge ($dm_{\rm bulge}$), the "contributing" mass ratio $\mu'_{\rm gal}$ is defined by $\mu_{\rm gal}$ of the merger that first made the mass into bulge (regardless of whatever merger ultimately brings it into the final galaxy). This quantity answers the question "what kind of merger destroyed the progenitor disks of these galaxies?" or "what kind of merger created most bulges in the first place?".

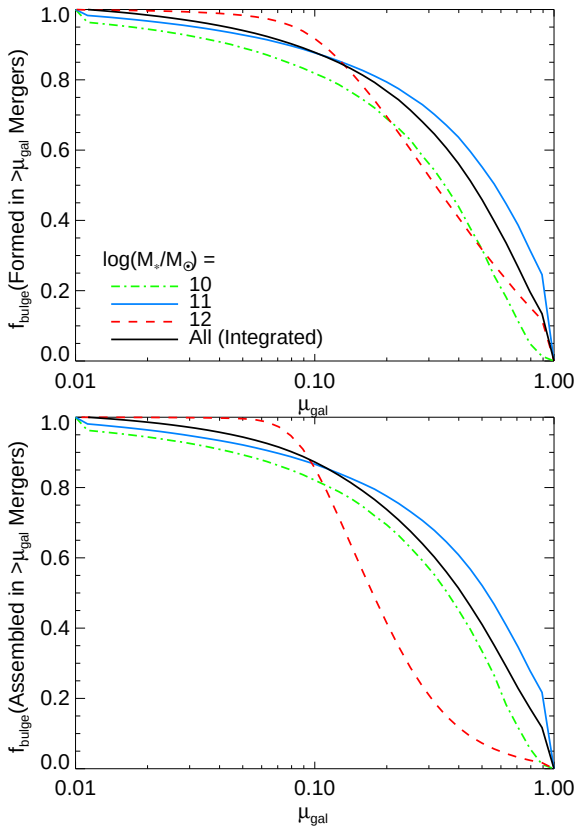

FIG. 8.— *Top:* Cumulative contribution to original *formation* of spheroid mass density from mergers of different mass ratios, for galaxies of given stellar mass at $z=0$ (as in Figure 1). "Integrated" curve refers to the integral over all bulge masses (net contribution to global spheroid mass density). *Bottom:* Same, but showing the contribution to the integrated spheroid *assembly*. Major mergers dominate near $\sim L_*$; minor mergers become more important at lower/higher masses. Assembly by minor dry mergers (of bulges first formed in more major mergers) occurs at the highest masses.

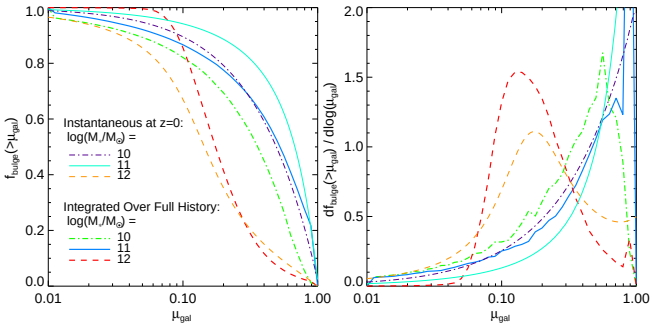

FIG. 9.— As Figure 8 (assembly), comparing the full result to an instantaneous calculation from convolving the $z = 0$ HOD of Wang et al. (2006) with instantaneous $z = 0$ merger rates. Because the *shapes* of the merger rate versus $\mu_{\rm halo}$ and $M_{\rm gal}(M_{\rm halo})$ functions do not evolve strongly with redshift, both yield similar results.

Second, assembly: we can define $f_{\rm bulge}(>\mu_{\rm gal})$ as the fraction of bulge mass *assembled* into the main branch of the galaxy by mergers with mass ratios $> \mu_{\rm gal}$. Here, we take Equation 4 where, for each parcel of mass, $\mu'_{\rm gal}$ is defined by $\mu_{\rm gal}$ of the merger that brought it into the main progenitor branch of the final galaxy. This answers the question, "what kind of merger brought most of the present-day bulge together?" or "what kind of merger has affected most of the mass in the bulge?".

Clearly, the two are equal if all bulge mass is formed "in situ" in the main progenitor – i.e. if the secondary galaxies have no pre-existing bulges. Indeed, at low masses, where most galaxies have little bulge, there is little difference.

At high masses, however, there is a dramatic difference. This makes sense: high-mass galaxies grow primarily by dry mergers. Galaxies first become bulge-dominated around $\sim L_*$, then assemble hierarchically. Since most bulge mass is first formed around $\sim L_*$, where we see bulge formation is dominated by major mergers, we obtain the result that bulges in high-mass galaxies are primarily *formed* in major mergers. However, as they grow in mass via dry mergers, minor mergers become increasingly important to the *assembly* of the most massive systems (minor mergers bring together bulges that have already been formed). Both definitions are clearly important and have their applications; however, because of e.g. the importance for remnant kinematics and growth histories, we will generally adopt the latter (assembly-based) definition in what follows.

The most important determinants of Figure 8 are the *shapes* (logarithmic slopes), not normalizations, of the halo merger rate versus $\mu_{\rm halo}$ and function $M_{\rm gal}(M_{\rm halo})$. These shapes evolve weakly with redshift, as such our results can be reasonably understood with a simple instantaneous calculation. Taking the $z = 0$ known $M_{\rm gal}(M_{\rm halo})$ alone, we can calculate the relative contribution to the differential growth rate of bulges at $z = 0$ as a function of mass (essentially this amounts to populating a $z = 0$ simulation with the observed HOD, and evolving it forward for some arbitrarily small amount of time, then calculating the relative importance of mergers as a function of their mass ratio). Figure 9 compares the results from this simple procedure with an integration over merger history (of course, without the full merger history, we can only define this in terms of the contribution to bulge assembly, not formation). There is little difference between the two. Because at any given stellar mass the most important mergers are those that happened while the system was relatively near that mass (not mergers that happened when the system was much lower mass, since those by definition will contribute little to the present total mass of the system), the "memory" of early formation or growth at low masses is effectively erased. This makes our results robust to details of the model at low masses and/or high redshifts, where empirical constraints are more uncertain.

5.2. *Dependence on Galaxy Mass*

We have shown how the relative importance of different mass ratio mergers depends on mass in Figures 8 & 9. Figure 10 summarizes these results. We plot the median $\langle\mu_{\rm gal}\rangle$ (specifically the mass-weighted median $\mu_{\rm gal}$, corresponding to the merger mass ratio above which 50% of the mass in bulges was assembled; i.e. where $f_{\rm bulge}(>\mu_{\rm gal}) = 0.5$ in Figure 9) as a function of stellar mass, at $z = 0$. We also plot the corresponding $\pm1\sigma$ and $10-90$% ranges. As demonstrated in Figure 9, similar results are obtained with an "instantaneous" calculation; in § 6, we show similar results varying a number of choices in the model.

As seen before, major mergers dominate near $\sim 10^{10} - 3\times 10^{11}\,M_\odot$, with minor mergers increasingly important at lower and higher masses. (In terms of the initial bulge formation, rather than assembly, the prediction would be the same but without the "turnover" at high masses – i.e. asymptoting to a constant $\langle\mu_{\rm gal}\rangle \sim 0.5$ at high masses.) Most of the variance comes from differences in merger histories at fixed mass. At all masses, the range of contributing mergers is quite large – there is always a non-negligible contribution from minor mergers with mass ratios $\sim 0.1-0.3$.

We stress that the turnover at high masses does not come because of fewer major mergers. In fact, we have shown explicitly that the number of major mergers in the primary history increases monotonically with galaxy mass. Rather, at high masses, the number of minor mergers increases even faster. Thus the *relative* importance of minor mergers is enhanced at the highest masses (picture for example the growth of a BCG via accretion of many satellites in a cluster). This is why the turnover would not appear if we made Figure 10 in terms of the mass ratios important for bulge formation, instead of bulge assembly. So we expect these systems to be more bulge dominated as compared to $\sim L_*$ galaxies, but with interesting second-order effects in e.g. their kinematics and light profile shapes that indicate the role of many minor mergers in their recent history.

5.3. *Dependence on Bulge-to-Disk Ratios*

Figure 11 examines how the distribution of contributing $\mu_{\rm gal}$ (in terms of bulge assembly) scales with the bulge-to-total stellar mass ratio B/T of galaxies. At fixed mass, galaxies with higher B/T are formed in preferentially more major mergers, and the trend is similar at all masses. This is the natural expectation: a more major merger yields a system with higher B/T. Because $\mu_{\rm gal}\,{\rm d}N_{\rm merger}/{\rm d}\log\mu_{\rm gal}$ is not quite flat in $\mu_{\rm gal}$ (rising to larger μ), and ~ 1 significant mergers are expected since $z \sim 2$ (i.e. at times when the galaxy is near is present mass), the local B/T will be dominated by the largest merger the system has experienced in recent times. Many objects all have some amount of bulge built by $\mu_{\rm gal} \sim 0.1$ mergers – the question is which will have larger mergers that convert more mass to bulge.

Figure 12 summarizes these results, showing the (mass-weighted) median merger mass ratio $\langle\mu_{\rm gal}\rangle$ contributing to bulge formation as a function of B/T at different stellar

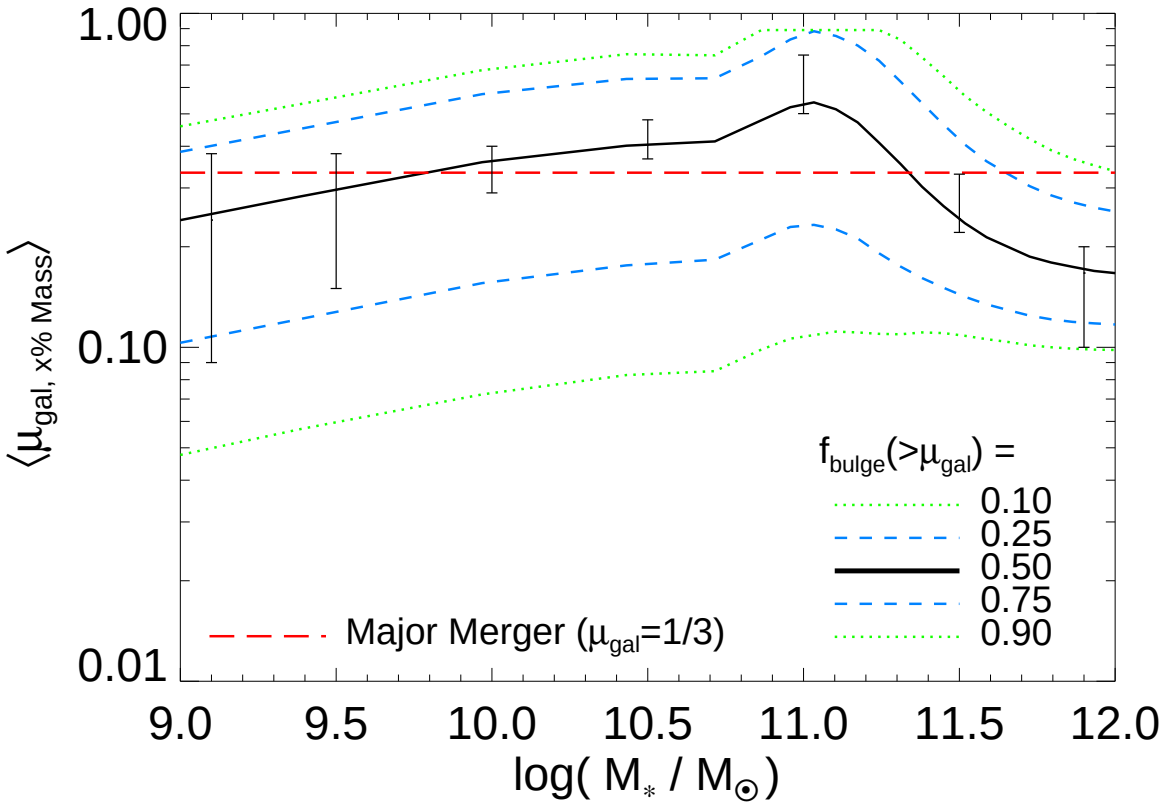

FIG. 10.— The relative importance of different mass ratios to bulge assembly as a function of $z = 0$ stellar mass. We plot the (mass-weighted) median $\mu_{\rm gal}$ contributing to the assembly of bulge mass density (defined as $\mu_{\rm gal}$ where $f_{\rm bulge}[>\mu_{\rm gal}] = 0.5$) as a function of stellar mass, along with the interquartile range and $10-90\%$ range (lines bracketing different ranges as labeled; horizontal dashed line denotes the standard "major merger" definition $\mu > 1/3$). Error bars show the range resulting from variations to the model (see § 6). Recall, the number of major mergers increases monotonically with mass; the decrease here at high mass is simply because the number of minor mergers increases yet more rapidly.

masses. At all masses, even masses where the *global* bulge population is predominantly formed in minor mergers, galaxies that are bulge-dominated (the E/S0 population) are predominantly assembled (and formed) in major mergers. In principle ten 1:10 mergers in a short time will form as much bulge as a single 1:1 merger. However, 1:10 mergers are *not* ten times more common, and as such are not an important or efficient channel for the formation of bulge-dominated galaxies. Recall that the average galaxy still experiences only ~ 1 minor 1:10 mergers since $z \sim 2$ (see Figure 3 & Stewart et al. (2008, 2009a)); the case of ten 1:10 mergers is then a $\sim 5-10\sigma$ outlier. Moreover, even if a system has several such mergers, they will be spaced widely in time (they essentially never occur simultaneously), so the galaxy disk will re-grow, reducing B/T after each and offsetting the bulge growth from mergers. In contrast, $\sim 1/2$ of all galaxies undergo a single 1:3 merger since $z \sim 2$; these will immediately form a large B/T system. In short, minor mergers are not *so much more common* than major mergers as to dominate the formation of high B/T systems.

This is also important for reproducing the existence of disks (especially "bulge-less" disks) – if minor mergers were so common as to dominate the formation of high B/T systems (if e.g. half of $\sim L_*$ galaxies had formed through the channel of ~ 10 rapid 1:10 mergers), it would be correspondingly much more rare for a system to have undergone very *few* 1:10 mergers, necessary to explain the existence of at least some significant number of low-mass systems with $B/T < 0.1$. Moreover, in practice any system with such an extreme merger history is likely to have also experienced an enhanced major merger rate – so the major mergers will still dominate bulge formation (it is unlikely to contrive an environment with so many $\sim 1:10$ mergers in a short time and no major mergers).

On the other hand, this implies that minor mergers do dominate the formation of bulges in *low* B/T galaxies (Sb/Sc/Sd galaxies). This is for the same reason – most galaxies have experienced ~ 1 1:10 merger in recent times ($z < 2$), whereas only some fraction have undergone more major mergers. The "traditional" scenario for bulge formation – early formation in a major merger, followed by subsequent re-growth of a disk by new cooling – is only responsible for a small fraction of the mass density in disk-dominated $B/T \lesssim 0.2$ systems. It is very rare that a system would have such an early major merger but then *not* have a later $\sim 1:10$ merger in the Hubble time required to grow the galaxy by a factor ~ 10 in mass.

These results are independent of all our model variations (§ 6), so long as we ensure that we reproduce a reasonable match to the observed HOD and halo merger rates. In fact, these conclusions appear to be quite general, similar to those found from other models that adopt different models for bulge formation in mergers (see e.g. Khochfar & Silk 2008; Weinzirl et al. 2009).

Figures 11 & 12 also show how, at fixed B/T, the contributing mass ratio distribution depends on stellar mass. At fixed B/T, the trend with mass is much weaker than seen comparing all galaxies as a function of mass (Figure 10). Moreover, the trend at fixed B/T appears to have an *opposite* sense: low-mass galaxies require *higher* mass ratio $\mu_{\rm gal}$ mergers to reach the same B/T. This is priarily a consequence of the dependence of gas fraction on stellar mass and the effects of gas

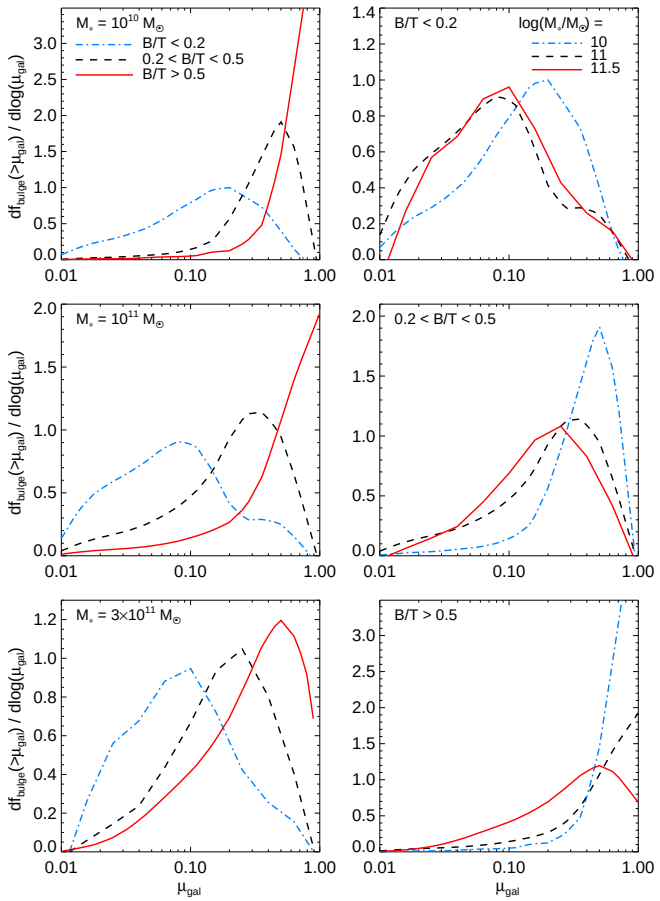

FIG. 11.— *Left:* Contribution of mergers of different $\mu_{\rm gal}$ to bulge assembly (as Figure 9; differential version), as a function of bulge-to-total ratio B/T at fixed galaxy mass. Line type denotes the final B/T value (as labeled), and each panel shows galaxies of a different mass. At all masses, more bulge-dominated systems are formed by more major mergers. Ellipticals and S0's are dominated by major merger remnants; late-type disk bulges are preferentially formed in situ in minor mergers. *Right:* Same, as a function of galaxy stellar mass at fixed B/T (lines denote different galaxy masses, panels show results for systems with different final B/T). At fixed B/T, the residual dependence on mass is weak; low-mass galaxies are more gas-rich, so require more major mergers to reach the same B/T.

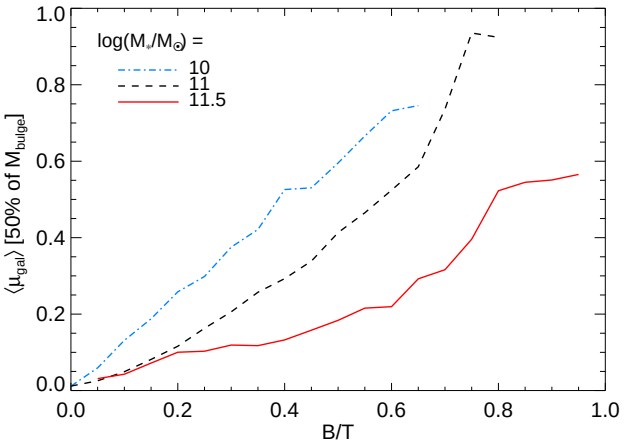

FIG. 12.— Summary of Figure 11: median mass ratio of mergers contributing to bulge growth (defined as in Figure 10) as a function of the final B/T and galaxy stellar mass (different lines). Roughly speaking, the correlation reflects the instantaneous scaling for a single merger, $B/T \propto \mu_{\rm gal}$ (as expected if galaxies grow in a manner such that the most recent mergers, at e.g. $z \lesssim 2$, are most important).

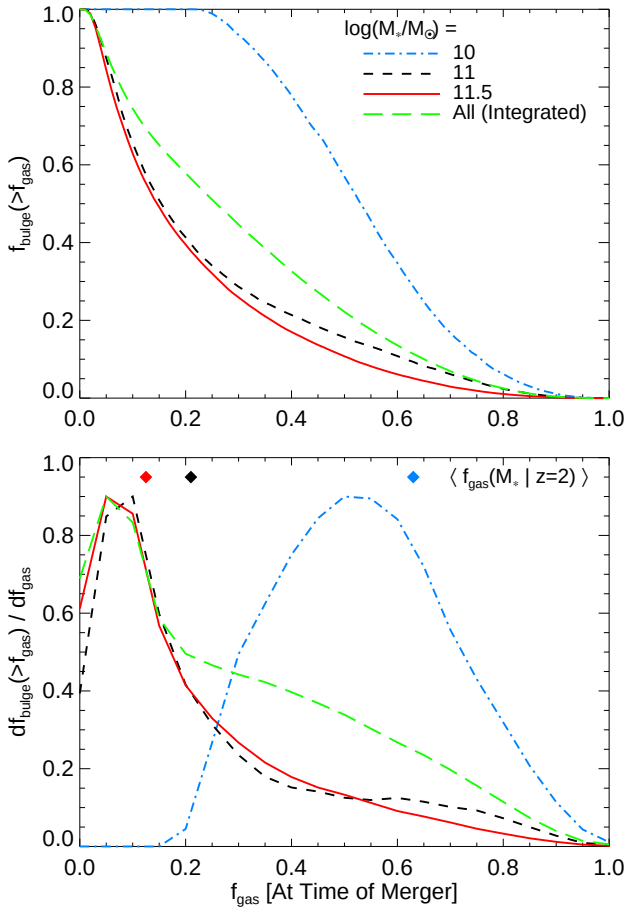

FIG. 13.— As Figure 11, but showing the contribution to bulge growth from mergers with different gas fractions $f_{\rm gas}$. *Top:* Integrated distribution (fraction of bulge mass formed in mergers with $f_{\rm gas}$ above the given value; lines show results at different stellar masses, with the "all" line integrated over the entire bulge mass function). *Bottom:* Same, in differential form (contribution per unit $f_{\rm gas}$). We compare the median $z = 2$ gas fractions of disks of the same mass (diamonds, color corresponds to the mass as labeled). To lowest order, the gas fractions of bulge-forming mergers simply reflect the gas fractions of disks at the time of merger ($z = 2$ is just representative; the distribution of merger times is broad). The bulge mass density is dominated by mergers with $f_{\rm gas} \sim 0.1-0.2$, with a tail towards more dissipational mergers in lower-mass systems.

on bulge formation (Figure 7). A low-mass galaxy, being very gas-rich, might require a major merger to even get to $B/T \sim 0.2$ (if, say, $f_{\rm gas} \sim 0.8$) – so low-mass systems will require more major mergers. On the other hand, mergers in a massive $\sim 10^{12}\,M_\odot$ system, being gas-poor ($f_{\rm gas} \lesssim 0.05$), will yield $B/T > 0.2$ for any mergers with $\mu_{\rm gal} > 0.2$; the $\sim 10^{12}\,M_\odot$ galaxies with low B/T (what few there are) must be those that had only minor mergers in the last few Gyr.

Overall, however, we wish to stress that systems with large B/T at low masses and low B/T at high masses are rare – *most* low mass systems, having low B/T, have had relatively more contribution to their bulge growth from minor mergers, and most higher mass systems, having high B/T, have had increasing contributions from major mergers.

5.4. *Dependence on Galaxy Gas Fractions*

Figure 13 compares the contribution to bulge formation from mergers not as a function of mass ratio, but as a function of the gas-richness of the merger, where $f_{\rm gas}$ is here defined as the sum gas-richness just before the merger ($= (M_{\rm gas,1} + M_{\rm gas,2})/(M_{\rm gal,1} + M_{\rm gal,2})$). In an integrated sense,

the most important gas fractions for bulge formation are $f_{\rm gas}\sim 0.1-0.2$.[22]. This agrees well with estimates from numerical simulations of the gas fractions required to form realistic $\sim L_*$ ellipticals (in terms of their profile shapes, effective radii and fundamental plane correlations, rotation and higher-order kinematics, isophotal shapes, triaxiality, and other properties; see e.g. Naab et al. 2006; Cox et al. 2006a; Jesseit et al. 2007, 2009; Hopkins et al. 2008c,a, 2009c)[23]. In a cosmological sense, it simply reflects the gas fractions of $\sim L_*$ disks, the progenitors of $\sim L_*$ ellipticals. We stress that this does not mean the bulges are made purely from this (relatively small) gas mass – rather, this represents the typical mass fraction formed in a central starburst in the bulge-forming merger; the majority of the bulge mass is formed via violent relaxation of the pre-merger disk stars.

As a function of mass, the typical merger contributing to bulge formation is more gas-rich at low masses. But as shown in Figure 13, this largely reflects the trend of gas fractions in late type or star-forming galaxies as a function of mass. At a given mass, in particular at the lowest masses where gas fractions can be sufficiently high as to significantly suppress bulge formation, there is a weak tendency for the dominant mergers contributing to bulge formation to be less gas-rich (since such mergers will, for the same mass ratio, form more bulge). However, the effect is not large.

An important check of this is that it reproduce the "dissipational" mass fraction in observed ellipticals, as a function of mass. This is the mass fraction of the spheroid formed in a dissipational starburst, rather than violently relaxed from the progenitor stellar disks. Being compact, this component is the primary element that determines the effective radii, profile shape, and ellipticity of a merger remnant. Hopkins et al. (2009a,e, 2008a) develop and test an empirical method to estimate the dissipational mass fraction in observed local ellipticals, and apply this to a wide range of observed ellipticals with a combination of HST and ground-based data from Kormendy et al. (2009) and Lauer et al. (2007). As shown therein, resolved stellar population studies yield supporting conclusions. Figure 14 shows these empirically inferred dissipational fractions as a function of mass, and compares the predictions from the models here. The agreement is reasonable. Similar conclusions are reached even by models with significantly different bulge formation prescriptions (Khochfar & Silk 2006). Note that the observed systems here are all classical bulges, appropriate for comparison to our predictions.

We also compare observed disk gas fractions. To lowest order, the dissipational fractions simply trace these gas fractions, but at low masses, the predicted and observed dissipational fractions asymptote to a maximum $\sim 0.3-0.4$. This is because angular momentum loss in the gas becomes less efficient at these high gas fractions; if the fraction of gas losing angular momentum scales as adopted here, then the dissipational fraction of the bulge formed from disks with gas fraction $f_{\rm gas}$ is not $\sim f_{\rm gas}$, but $\sim f_{\rm gas}/(1+f_{\rm gas})$, i.e. asymptoting to the values observed for all $f_{\rm gas}\sim 0.5-0.9$.

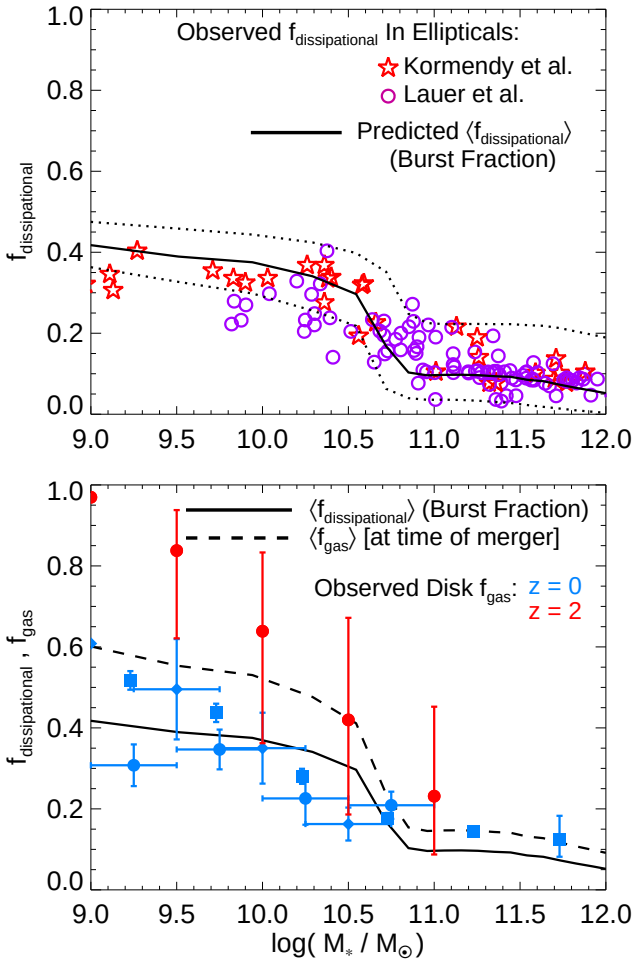

FIG. 14.— *Top:* Dissipational fraction (mass fraction of bulges formed in starbursts from gas that has lost its angular momentum in mergers, relative to the total – starburst plus violently relaxed former stellar disk – bulge mass) as a function of stellar mass (solid line is the predicted median; dotted the $\pm1\sigma$ scatter). We compare to empirically inferred $f_{\rm dissipational}$ from decomposition of high-resolution surface brightness profiles and kinematics of observed ellipticals, presented in Hopkins et al. (2009a,e) with samples from Kormendy et al. (2009) and Lauer et al. (2007). *Bottom:* Predicted dissipational fraction from above (solid line), and median gas fraction $f_{\rm gas}$ of mergers contributing to bulge growth (from Figure 13; dashed line), compared to observed disk gas fractions (from Figure 7; points in the same style, with values at $z=0$ and $z=2$ in blue and red, respectively). Dissipational fractions reflect the gas fractions of progenitor disks, but with an asymptotic upper limit of $f_{\rm dissipational}\sim 0.4$ that reflects the suppression of angular momentum loss in very gas-rich mergers.

5.5. *Redshift Evolution: Can Mergers Account for the Mass Density in Bulges?*

At all redshifts, the distribution of $\mu_{\rm gal}$ contributing to bulges is similar to that at $z=0$, shown in Figure 15. The only significant evolution is that the "turnover" in $\langle\mu_{\rm gal}\rangle$ at high masses for the mass ratios contributing to bulge assembly (Figure 10) becomes less pronounced and moves to higher masses. Technically, this relates to how $M_{\rm gal}(M_{\rm halo})$ (empirically constrained) evolves, but physically it is simply understood: at higher redshifts, "dry" assembly is less important, so the assembly $\langle\mu_{\rm gal}\rangle$ increasingly resembles the formation $\langle\mu_{\rm gal}\rangle$ (Figure 8). By $z\sim 2$, there is no difference – dry assembly is negligible, and all high-mass, high-B/T systems are preferentially formed in major mergers.

[22] Recall, this is the gas fraction *at the time of the merger*, and can be different from the "initial" gas fraction at the beginning of an interaction, depending on e.g. the efficiency of star formation and stellar feedback. For example, in hydrodynamic simulations of idealized mergers without ongoing continuous accretion, a gas fraction at the time of merger of $\sim 0.1-0.2$ corresponds to an "initial" gas fraction ~ 2 Gyr before merger of $\sim 0.3-0.4$.

[23] In fact, only mergers with these properties have been shown to yield a good match to these quantities: mergers with significantly less or more gas, as well as secular instabilities and dissipational collapse have been shown to yield remnants with properties unlike observed ellipticals.

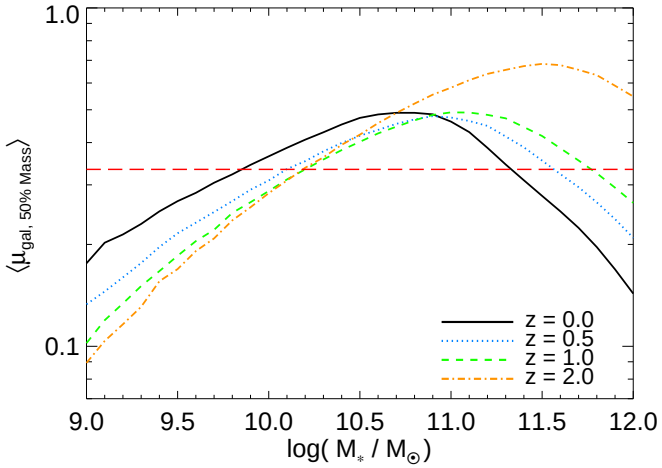

FIG. 15.— As Figure 10, showing the (mass-weighted) median mass ratio $\mu_{\rm gal}$ contributing to bulge assembly as a function of mass for samples at different observed redshifts, $z = 0-2$ (different lines, as labeled; again the red horizontal line denotes the traditional major merger definition $\mu > 1/3$). The qualitative trends are similar; at high redshifts the break/turnover moves to higher masses.

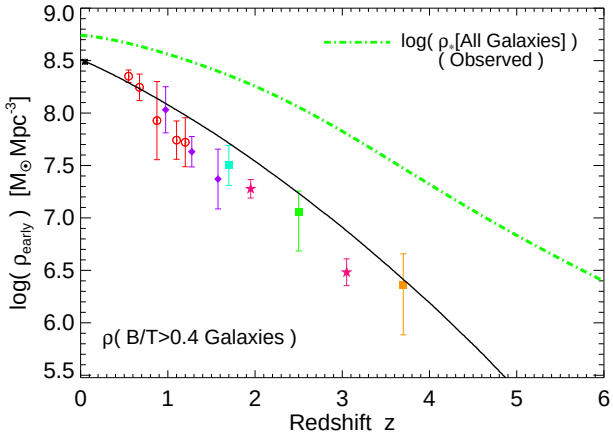

FIG. 16.— Predicted integrated mass density in bulge-dominated galaxies ($B/T > 0.4$; black solid line) as a function of redshift, compared to observations (points). Observations are from the morphologically-selected samples of Bell et al. (2003, black $\times$), Bundy et al. (2005, 2006, red circles), Abraham et al. (2007, violet diamonds), and Daddi et al. (2005, cyan square), and color-selected samples of Labbé et al. (2005, green square), van Dokkum et al. (2006, orange square), and Grazian et al. (2007, magenta stars). We compare the total stellar density observed (green dot-dashed line; Hopkins & Beacom 2006). Increasing gas fractions and cooling rates at high redshift suppress the bulge mass density relative to the total stellar mass density. The predicted number of mergers is sufficient to account for the $z = 0$ and high-redshift evolution in the global bulge mass budget, but with factor ~ 2 uncertainties.

Given these predicted merger rates and B/T distributions, we also obtain a prediction for the mass density in bulge-dominated galaxies as a function of redshift. Figure 16 compares the redshift evolution of the bulge mass density to that observed. [24] The agreement is good: not only are there a sufficient number of major mergers to account for the observed merger fractions, but also to account for the observed buildup of the bulge population with redshift. This should not be surprising, given the agreement with observed merger fractions demonstrated in § 4.2 above; Hopkins et al. (2007a, 2008b), Bundy et al. (2009), and Bell et al. (2006a) have demonstrated that observed major merger fractions are sufficient, within a factor ~ 2, to account for the observed growth of the bulge population over the same redshift interval (given the observable lifetime calibrations that we adopt in § 4.2; note that some of these works use different merger timescale estimates and reach different conclusions, but they are consistent using a *uniform*, simulation-calibrated timescale). Similar results as a function of galaxy morphology are suggested by local observations (e.g. Darg et al. 2009a). Likewise the agreement between the predicted integrated number of mergers and various observational estimates suggests this is plausible (de Ravel et al. 2009; Conselice et al. 2009; Lin et al. 2008).

For a more detailed comparison, as a function of e.g. galaxy stellar mass, we refer to Hopkins et al. (2009g), who use the same merger rates as modeled here to predict e.g. the morphology (B/T)-mass relation and bulge/disk mass functions as a function of redshift. Provided proper account of galaxy gas fractions is taken, good agreement is obtained. Stewart et al. (2009b) perform a similar calculation (with a basic criteria for bulge formation), with merger rates in close agreement as a function of galaxy mass to those measured observationally in Bundy et al. (2009), and obtain similar good agreement with the bulge mass function as a function of redshift. They actually find that bulge mass is somewhat overproduced, without accounting for the role of gas-rich mergers. Hopkins et al. (2008d) and Hopkins et al. (2008b) consider a range of model parameter space (with several of the specific model variations discussed in § 6) and perform similar calculations; they explicitly show the predicted spheroid mass function and mass fraction as a function of stellar mass, halo mass, environment, and redshift, for the different models considered. They likewise conclude that, for all the model variations considered (with scatter in merger rates as a function of mass similar to that discussed below), good agreement with the mass function and mass density of classical bulges, at masses $> 10^{10}\,M_{\odot}$, is obtained. At lower masses, however, uncertainties grow rapidly.

Relative to the *total* stellar mass density, the mass density in bulge-dominated galaxies decreases with redshift. This is discussed in detail in Hopkins et al. (2009g), but the reason is simply that at higher redshifts, higher gas fractions suppress bulges (and the suppression moves to higher mass, relative to the galaxy mass function break. This trend agrees with that observed and is not trivial (models neglecting the importance of gas-richness in affecting bulge formation efficiency in mergers, for example, may predict the opposite).

5.6. *Analytic Fits*

It is convenient to fit the distribution of merger mass ratios contributing to bulge formation at a given mass. The average $\mu_{\rm gal}$ contributing to bulge *assembly*, i.e. $\langle\mu_{\rm gal}\rangle$ where $f_{\rm bulge}(>\mu_{\rm gal}) = 0.5$, as a function of $z = 0$ galaxy stellar mass M_* (Figure 10) can be approximated as

$$\langle\mu_{\rm gal}\rangle = \frac{1}{(M_*/10^{11}M_{\odot})^{-0.5} + (M_*/10^{11}M_{\odot})^{0.8}}\,. \quad (11)$$

[24] Specifically, we plot the mass density in bulge-dominated galaxies, which is not the same as the absolute mass density in all bulges, but is closer to the observed quantity. At high redshifts $z > 1.5$ observed morphologies are ambiguous; we show the mass density in passively evolving red galaxies as a proxy. This may not be appropriate, but at $z < 1$ the two correspond well, and the compactness, size, and kinematics of the "passive" objects do appear distinct from star-forming objects (Kriek et al. 2006; Toft et al. 2007; Trujillo et al. 2007; Franx et al. 2008; Genzel et al. 2008). Also, the observations in some cases do not distinguish "classical" and "pseudo" bulges; but as we discuss in § 7, the latter where measured appear to contribute only $\sim 10\%$ of the mass density.

If instead the $\langle\mu_{\rm gal}\rangle$ contribution to bulge *formation* is desired, a similar formula applies, but with a weaker turnover at high M_*, i.e.

$$\langle\mu_{\rm gal}\rangle = \frac{1}{(M_*/10^{11}M_\odot)^{-0.5}+(M_*/10^{11}M_\odot)^{0.2}}\ . \quad (12)$$

In greater detail, Figures 11-12 demonstrate that the typical $\langle\mu_{\rm gal}\rangle$ contributing to bulge assembly depends on the bulge mass fraction B/T at a given mass. As a bivariate function of B/T and mass, $\langle\mu_{\rm gal}\rangle$ can be approximated by:

$$\langle\mu_{\rm gal}\rangle = \left[\frac{B}{T}\right]\times\frac{1}{1+(M_*/10^{11}M_\odot)^{0.5}}\ . \quad (13)$$

Finally, knowing $\langle\mu_{\rm gal}\rangle$, we find that the complete distribution $f_{\rm bulge}(>\mu_{\rm gal})$ (e.g. Figure 8) can be simply approximated by

$$f_{\rm bulge}(>\mu_{\rm gal}) = (1-\mu_{\rm gal})^{\gamma} \quad (14)$$

where (since $f_{\rm bulge}(>\langle\mu_{\rm gal}\rangle)=0.5$), the slope γ is trivially related to $\langle\mu_{\rm gal}\rangle$ as:

$$\gamma = \frac{-\ln 2}{\ln(1-\langle\mu_{\rm gal}\rangle)}\ . \quad (15)$$

6. HOW ROBUST ARE THESE CONCLUSIONS? A COMPARISON OF MODELS

The relative importance of e.g. minor and major mergers in bulge assembly owes to the combination of reasonably well-determined halo merger rates and halo occupation statistics. Nevertheless, there are still uncertainties in this approach. We therefore examine how robust the conclusions here are to a variety of possible model differences. A much more detailed investigation of e.g. differences in predicted merger rates between semi-empirical models, semi-analytic models, and simulations will be the subject of a companion paper (Hopkins et al. 2009f). Here, we wish to examine differences arising within the semi-empirical framework.

Figures 17-18 compare our "default" model with a number of alternatives. For each alternative, we show the the merger rate as a function of redshift, and the integrated contribution of different mass ratios $f_{\rm bulge}(>\mu_{\rm gal})$ to bulge assembly (integrated over all bulge masses). For the merger rates, we also compare with the observational constraints: the dotted region in the Figure shows the approximate $\pm1\,\sigma$ allowed range from the observational compilation in Figures 4-5 (fitting a piecewise broken power-law to the observations), given the merger lifetime calibrations discussed in § 4.2.

The model variations we consider include:

6.1. *Halo Occupation Models*

Here, we consider an otherwise identical model, but adopt a different set of halo occupation constraints to determine $M_*(M_{\rm halo})$ (for now, we keep $M_{\rm gas}(M_*)$ fixed, but varying that is very similar to varying $M_*(M_{\rm halo})$). First, our default model, using the fits from Conroy & Wechsler (2009). Second, the first to $M_*(M_{\rm halo})$ and its scatter for central and satellite galaxies from the observed SDSS clustering at $z=0$ (Wang et al. 2006); here, we simply adopt the $z=0$ fit at all redshifts – we do not allow for evolution. Third, assigning galaxies to halos and subhalos based on a monotonic rank-ordering method (see Conroy et al. 2006), fitting to the redshift-dependent stellar mass function from Fontana et al. (2006). Fourth, the same, with the mass functions from Pérez-González et al. (2008b).

We have also considered various fits directly taken from other sources, including Yan et al. (2003); Cooray (2005, 2006); Conroy et al. (2006, 2007); Zheng et al. (2007) and Pérez-González et al. (2008a); these lie within the range shown in Figure 17. Using the HOD predicted by semi-analytic models, at least for central galaxies, also appears to give similar results (we have compared the results in Croton et al. 2006; Bower et al. 2006; de Lucia & Blaizot 2007); given that these models are constrained to match the observed stellar mass function, this appears to be sufficient for the level of convergence shown.

6.2. *Merger Timescales*

In our "default" model, we assume a delay between halo-halo and galaxy-galaxy mergers, given by the dynamical friction time calibrated to simulations in Boylan-Kolchin et al. (2008). We now allow this to vary according to five different scalings, described in detail in Hopkins et al. (2008d). **(a)** Dynamical Friction: the traditional dynamical friction time, using the calibration from numerical simulations in Boylan-Kolchin et al. (2008) (see also Jiang et al. 2008). **(b)** Group Capture: the characteristic timescale for pair-pair gravitational capture in group environments, calibrated to simulations following Mamon (2006) (see also White 1976; Makino & Hut 1997) **(c)** Angular Momentum Capture: as group capture, but considering capture in angular momentum space rather than gravitationally, following Binney & Tremaine (1987). **(d)** Gravitational Cross-Sections: similar to the group capture timescale, this is the timescale for gravitational capture between passages in e.g. loose group or field environments, calibrated from simulations in Krivitsky & Kontorovich (1997). **(e)** No Delay: simply assuming galaxy-galaxy mergers occur when their parent halo-halo mergers do.

Although the dynamical friction time is most commonly adopted in e.g. semi-analytic models, each of these timescales depends on certain assumptions and is relevant in different regimes. A dynamical friction time is appropriate for a small, dense satellite at large radii; it becomes less so at small radii. A group capture or gravitational capture cross section, on the other hand, is appropriate for collisions in small groups or field environments where "inspiral" is not well-defined. The angular momentum calibration from Binney & Tremaine (1987) is more appropriate for satellite-satellite mergers. In any case, we see the choice makes little difference to our conclusions. And the range between these choices is generally much larger than other, more subtle details (e.g. allowing for continuous satellite mass loss in inspiral, or resonant baryonic effects that speed up the coalescence). The reason is simply that we are largely focused on fairly major mergers, for which the merger time is short relative to the Hubble time. The rate-limiting step is the accretion of such a companion, not the inspiral time.

6.3. *SubHalo Mass Functions/Substructure-Based Methodologies*

Instead of using a halo-halo merger rate with some "delay" applied, we can attempt to follow subhalos directly after the halo-halo merger, and define the galaxy-galaxy merger when the subhalos are fully merged/destroyed. This will self-consistently allow for some distribution of merger times owing to e.g. a range of orbital parameters, and will include satellite-satellite mergers (neglected in our default model),

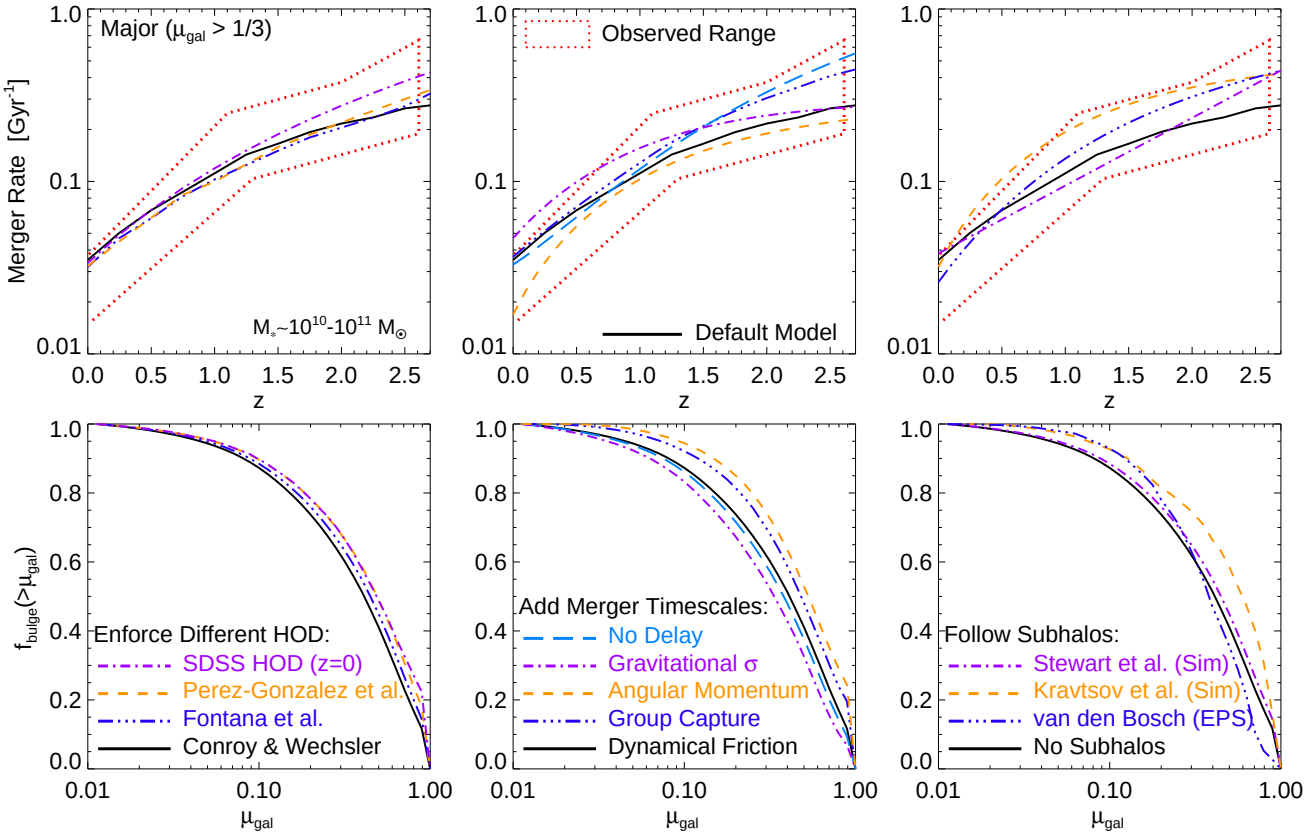

FIG. 17.— *Top:* Predicted major merger rate ($\mu_{gal} > 1/3$), varying the assumptions in the models (different lines). Black line is the "default" model assumption. Red dotted range is the approximate range allowed by observations (the compiled points in Table 1 & Figure 4; for clarity, we show the range of these points rather than each individual measurement). *Bottom:* Corresponding cumulative contribution of different mass ratio mergers to the assembly of the bulge mass density (as Figure 8, integrated over all bulge masses). *Left:* Changing the halo occupation constraints: the three cases from Figure 3 are shown, together with adopting the $z = 0$ SDSS fits from Wang et al. (2006) at all redshifts. *Center:* Changing the merger timescale between halo-halo and galaxy-galaxy merger: using dynamical friction times (calibrated in Boylan-Kolchin et al. 2008); angular momentum-space capture cross sections from Binney & Tremaine (1987); collisional group capture cross sections from Mamon (2006); gravitational capture cross-sections for field/small group crossings from Krivitsky & Kontorovich (1997); or no delay. *Right:* Tracking subhalos to assign merger times or using subhalo mass functions instead of halo merger trees as a starting point: using the subhalo merger trees from cosmological simulations in Stewart et al. (2009a); adopting the subhalo mass functions from simulations in Kravtsov et al. (2004); or the same from extended Press-Schechter trees constructed following van den Bosch et al. (2005).

which Wetzel et al. (2009a) show can be important at the $\sim 10-20\%$ level independent of halo mass.

Here, we compare our default model to those obtained tracking the halo+subhalo populations in cosmological simulations from Stewart et al. (2009a) (populating subhalos according to our default HOD). Wetzel et al. (2009a,b) also analyze subhalo merger rates, with a different methodology. They reach similar conclusions, but with a systematic factor $\sim 1.5-2$ lower merger rate. As they discuss, this is quite sensitive to how one defines e.g. subhalo versus friends-of-friends group masses; some of those choices of definition will be "normalized out" by the appropriate HOD (renormalized for whatever subhalo populations are identified in a simulation so as to reproduce the observed clustering and mass functions), but it also reflects inherent physical uncertainties in the instantaneous mass and time of subhalo merger.

We also compare with the results using the different subhalo-based methodology described in Hopkins et al. (2008d) (essentially, beginning from the subhalo mass function constructed from cosmological simulations and evolving this forward in short time intervals after populating it, at each time, according to the HOD constraints). We compare two different constructions of the subhalo mass functions: that from cosmological dark-matter only simulations in Kravtsov et al. (2004) (see also Zentner et al. 2005) and that from the extended Press-Schechter formalism coupled to basic prescriptions for subhalo dynamical evolution, described in van den Bosch et al. (2005). Alternative subhalo mass functions from e.g. De Lucia et al. (2004); Gao et al. (2004); Nurmi et al. (2006) are consistent.

6.4. *Halo Merger Rates*

We can next vary the halo-halo merger rates adopted. Our default model uses the merger rates in Fakhouri & Ma (2008b), calibrated from the Millenium dark-matter only cosmological simulation (Springel et al. 2005c, 2006). Since we use the full history, this is equivalent to the "per progenitor" merger rates defined from the same simulation in Genel et al. (2008). An alternative dark-matter simulation, of comparable resolution, with halo merger rates determined using a different methodology, is described in Stewart et al. (2009a). Another is found in Gottlöber et al. (2001) (see also Kravtsov et al. 2004; Zentner et al. 2005); they quantify the fit separately to field, group, and cluster environments.

We can also compare with the merger rates from Maller et al. (2006), determined from cosmological hydrodynamic simulations. Although it is well known that, without proper implementations of feedback from various sources, cosmological hydrodynamic simulations yield galaxies that suffer from overcooling (and do not reproduce the observed

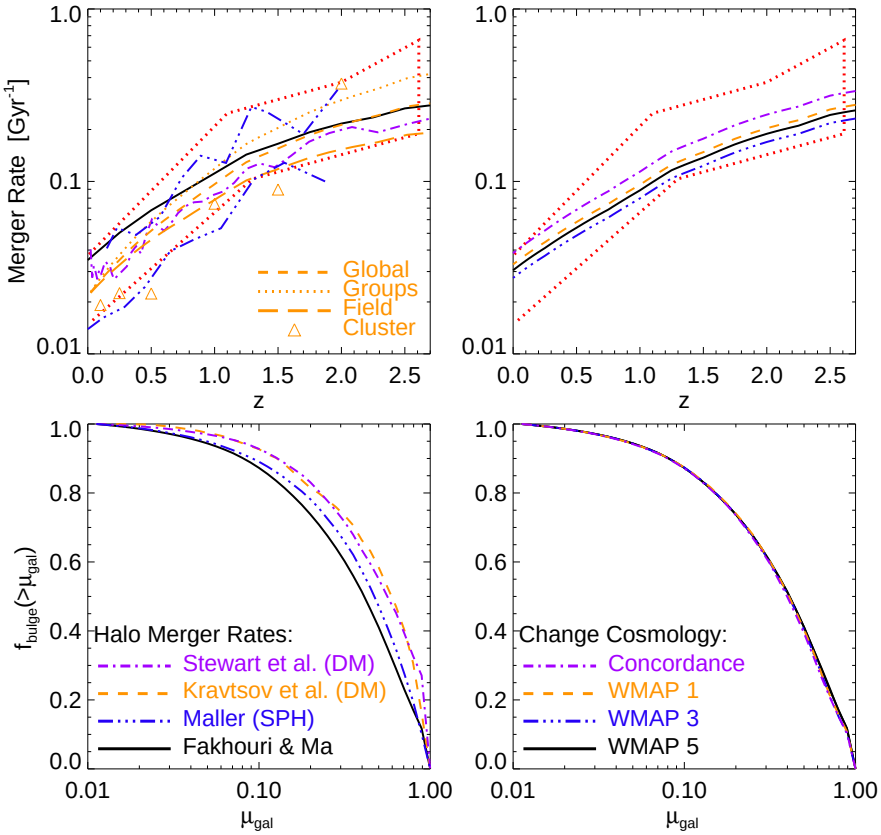

FIG. 18.— Figure 17, continued. *Left:* Changing the halo-halo merger trees: our default choice from the Millenium simulation analyzed in Fakhouri & Ma (2008b); numerical trees from an alternative high-resolution cosmological simulation (Stewart et al. 2008, 2009a); cosmological DM only simulations of field, group, and cluster environments (as labeled; Gottlöber et al. 2001); or merger rates from cosmological SPH simulations (tracking galaxy-galaxy mergers but still re-populating them appropriately for the observed HOD; Maller et al. 2006, upper and lower correspond to their high and medium-mass primary sample, respectively). *Center:* Changing the cosmology: our default WMAP5 (Ω_m, σ_8)=(0.27, 0.81) cosmology, versus a WMAP1 (0.27, 0.84), WMAP3 (0.27, 0.77), and "concordance" (0.3, 0.9) cosmology.

halo occupation statistics), the galaxies in these simulations can still serve as "tracers" of halos and subhalos. This provides a means to avoid the considerable ambiguities in defining a halo merger (moreover in considering the delay between halo-halo and galaxy-galaxy mergers). Although the galaxy *masses* may not be correct, they are still tracers of where in the halo real galaxies should be, and therefore can be used to measure the halo merger rate. We do so by recalculating their merger rates after re-populating the galaxies appropriately (essentially renormalizing their predicted mass function to match that observed).

6.5. *Cosmological Parameters*

We can also vary the cosmological parameters and see if this makes a significant difference to our conclusions. We consider four sets of cosmological parameters: a "concordance" model with $(\Omega_{\rm M}, \Omega_\Lambda, h, \sigma_8, n_s)$=$(0.3, 0.7, 0.7, 0.9, 1.0)$, the WMAP1 $(0.27, 0.73, 0.71, 0.84, 0.96)$ results of Spergel et al. (2003), WMAP3 $(0.268, 0.732, 0.704, 0.776, 0.947)$ (Spergel et al. 2007), and WMAP5 $(0.274, 0.726, 0.705, 0.812, 0.96)$ (Komatsu et al. 2009). It is prohibitively expensive to re-run the simulations for each case, and moreover the qualitative behavior is not expected to change (seen in e.g. lower-resolution dark-matter simulations). We simply renormalize the halo masses at all times to match the halo mass function and accretion history appropriate for the revised cosmological parameters (see e.g. Neistein et al. 2006) – the dominant effect is the predicted halo mass function shifting to higher masses with larger σ_8. However, because we use a halo occupation-based approach, the model is re-normalized to yield the same observed galaxy mass function and clustering, so these differences are largely normalized out. Elahi et al. (2008) show that the quantity of greatest importance for our conclusions, the normalized substructure mass function or (equivalently) dimensionless merger rate (mergers per halo per Hubble time per unit mass ratio) is almost completely independent of cosmological parameters including e.g. the power spectrum shape and amplitude over the range of variations here (not until one goes to much larger effective $n_s \sim 3$ does one see this function change shape).

6.6. *Bulge Formation Prescriptions*

We can also consider variations in the physical prescription by which bulge mass is formed in mergers. Obviously this will not change the merger rates, but it could change the relative importance of mergers of different mass ratios. However, we are tightly constrained by the results of N-body simulations; since the physics determining gas angular momentum loss and violent relaxation are predominantly gravitational, there is little uncertainty in how much bulge should be formed in a given merger (given the appropriately normalized initial conditions of interest). Still, there are some differences in fitted prescriptions: we have re-calculated the results from our default model according to the approximate results of simulations from Naab & Burkert (2003) and Naab et al. (2007),

as well as Bournaud et al. (2005) and di Matteo et al. (2007). We have also used the fits to the same suite of simulations in Hopkins et al. (2009b) as presented in Cox et al. (2006b) and Cox et al. (2008). Note that the results in several of these works do not necessarily include a complete survey of parameters such as e.g. mass ratio, orbital parameters, and gas fraction; where not given we interpolate between the results presented based on the model outlined in Hopkins et al. (2009b). In any case, the differences in quantities such as the absolute bulge mass (especially in gas-rich, low mass systems) and dissipational fractions (fraction of mass formed in starbursts, rather than violently relaxed from stellar disks) of ellipticals can be non-negligible, but the relative contribution of major and minor mergers is almost identical.

This will be true, it turns out, in any model where the amount of bulge formed in a given merger scales roughly in linear fashion with the mass ratio. As such, even highly simplified models which ignore the role of gas fraction and orbital parameters, and/or only violently relax the primary in major mergers (but do destroy the secondary in minor mergers), will still obtain the same qualitative features in $f_{\rm bulge}(>\mu_{\rm gal})$; see e.g. Khochfar & Silk (2006).

6.7. *Combinations of the Above: Typical "Scatter"*

We have considered various permutations of the above models, amounting to ~ 700 total models; our conclusions are robust to these combinations. The interquartile range between this sampling of models lies within the observationally allowed range in terms of the merger rate, and yields very little scatter in $f_{\rm bulge}(>\mu_{\rm gal})$.

To the extent that comparison of these models can be considered "scatter" or reflective of uncertainties in the theoretical predictions, the corresponding typical "uncertainties" are as follows: around $\sim L_*$ and at slightly higher masses, uncertainties are small – a factor of ~ 1.5 in merger rates (at $z<2$; uncertainties grow at higher redshifts as in Figure 3) and smaller in $f_{\rm bulge}(>\mu_{\rm gal})$, with $f_{\rm bulge}(\mu_{\rm gal}>1/3)\sim 60-80\%$. At factors less than a few higher and lower masses, these uncertainties increase to a factor ~ 2 in merger rate, and factor ~ 1.5 in the importance of major versus minor mergers. At much lower masses ($\sim 10^9 M_\odot$), uncertainties in both grow rapidly – here, the halo occupation statistics are not strongly constrained. Moreover, $\mu_{\rm gal}$ is the *baryonic* (not just stellar) mass ratio, and systems at these masses are increasingly gas-dominated, so uncertainties in $M_{\rm gas}(M_*)$ can strongly affect our predictions.

7. DISCUSSION

7.1. *Approach*

We have used an extensive set of models to examine galaxy-galaxy mergers and to identify robust predictions for the relative importance of mergers of different mass ratios for bulge formation. Although halo-halo merger rates have been relatively well-understood, mapping halo-halo mergers to galaxy-galaxy mergers is not trivial. There can be significantly more or fewer major or minor galaxy-galaxy mergers, relative to halo-halo mergers; likewise, bulge growth can be dominated by preferentially more major or minor mergers than the growth of the host halo.

However, there is hope. Numerical simulations are converging in predicting how the efficiency of bulge formation scales with merger mass ratio (and what the "appropriate" mass ratio to use in these calculations should be), giving a straightforward set of predictions for how much bulge should be formed in a given galaxy-galaxy encounter. To lowest order, the amount of bulge formed scales linearly in the merger mass ratio, close to the maximal efficiency possible for minor mergers (Hopkins et al. 2009b).

Meanwhile, observations are converging on relatively tight constraints on halo occupation models: namely, the stellar and gas mass of the average galaxy hosted by a halo/subhalo of a given mass. The correlation between galaxy stellar mass and halo mass is monotonic and, to lowest order, amounts to a simple matched rank-ordering of the two, with small scatter (e.g. Conroy et al. 2006).

7.2. *Conclusions*

This convergence makes the time ripe to examine the consequences of galaxy-galaxy mergers on bulge formation. To good approximation, the salient features of the merger rate distribution can be captured by convolving the theoretically determined halo-halo merger rate with the empirically determined halo occupation statistics. Given this simple, well-constrained approach, there are some robust predictions that are insensitive to most if not all model details:

(1) *Major-mergers ($\mu_{\rm gal}>1/3$) remnants dominate the integrated mass density of merger/interaction-induced bulges at all redshifts* (Figures 8-11). Minor mergers ($1/10<\mu_{\rm gal}<1/3$) do contribute a significant, albeit not dominant, fraction ($\sim 30\%$) to the assembly of the total mass density. More minor mergers $\mu_{\rm gal}<1/10$ are not important (contributing $<5-10\%$).

(2) This statement is significantly mass-dependent (Figures 9-10). Although the relative major/minor contribution to halos is nearly mass-independent, the mass-dependent HOD shape leads to a galaxy mass dependence: major mergers strongly dominate bulge production around $\sim L_*$ (where most of the bulge and stellar mass density of the Universe lies). At masses $\ll L_*$, merger rates at all mass ratios are suppressed, and minor mergers are relatively more important (since $M_{\rm gal}\propto M_{\rm halo}^2$ at these masses, approximately, a 1:3 halo-halo merger becomes a 1:9 galaxy-galaxy merger; so all mergers are shifted to lower mass ratio, suppressing the number at some fixed $\mu_{\rm gal}$ and relatively suppressing major mergers). At higher masses $\gtrsim L_*$, merger rates are higher, and major mergers are relatively more important (here $M_{\rm gal}\propto M_{\rm halo}^{1/2}$, so a 1:9 halo-halo merger becomes a 1:3 galaxy-galaxy merger; making mergers at all significant mass ratios more abundant and relatively increasing the importance of major mergers). This is true until $\gtrsim$ a few L_*, where minor mergers again become relatively more important owing to the rapid dropoff in the number of "major" companions (equivalently, since most of the galaxy mass is concentrated near $\sim L_*$, most of the incoming mass density is weighted near this region as well, which is a major merger at $\lesssim$ a few L_* and minor merger above). These trends are quite general, and the relative "increased weight" of major mergers will occur wherever the "mass-to-light ratio" or formation efficiency $M_{\rm halo}/M_{\rm gal}$ has a minimum ($\sim L_*$).

(3) For massive galaxies, there is a difference between the mass ratios important for bulge *formation* (the mergers which initially converted some disk mass into bulge mass) and those important for bulge *assembly* (the mergers that

brought together the present-day bulge from any combination of pre-existing bulges and/or disks). At low masses, the two are equivalent (they are only different where "dry mergers" are significant). At high masses, the description above applies to assembly. Most mergers onto $\gg L_*$ systems are of already bulge-dominated galaxies (i.e. dry), systems which first turned their disk mass into bulge ("formed" the bulges) at progenitor masses near $\sim L_*$, where major mergers are most efficient. As a consequence, most bulge mass at all $> L_*$ masses is *formed* in major mergers (albeit again with non-negligible contributions from minor mergers); however, bulges are assembled in increasingly minor (dry) mergers at larger masses.

(4) The relative importance of major and minor mergers is also significantly morphology-dependent (Figures 11-12). Bulge-dominated (E/S0 or $B/T \gtrsim 0.4$) galaxies are preferentially formed in major mergers; later-type (Sb/c/d or $B/T \lesssim 0.2$) galaxies are preferentially formed in minor mergers. Despite the fact that simulations show that e.g. ten 1:10 mergers can yield just as much bulge mass as one 1:1 merger, cosmological models show that they are *not* ten times more common. Moreover, this many minor mergers would have to happen in a time much less than a Hubble time in order to successfully build a bulge-dominated galaxy, and this scenario is very unlikely (even at high redshift; minor merger rates may increase, but so do major merger rates). However, since just one or two 1:10 mergers are sufficient to account for a $B/T < 0.2$ bulge, this is a common formation channel for small bulges, in particular more common than a major merger at high redshifts that destroys the entire disk followed by a factor of ~ 10 subsequent disk re-growth (even if this occurred, it would take $\sim$ a Hubble time, in which time a 1:10 merger would be very likely, and that merger would then dominate the final bulge mass). To lowest order, bulges of systems of bulge-to-total ratio B/T are characteristically formed in mergers of mass ratio $\mu_{\rm gal} \sim B/T$ (Equation 13).

(5) Gas-richness, with high gas fractions $f_{\rm gas} \gtrsim 0.5$, can dramatically suppress the *global* efficiency of bulge formation (from mergers at all mass ratios), and the important implications of this for establishing the morphology-mass relation and allowing for a significant population of low B/T systems is discussed in Hopkins et al. (2009g) and Stewart et al. (2009b). However, it does not affect the merger rate, and because the effects are not mass ratio-dependent, it does not significantly affect the relative importance of major/minor mergers. Because low-mass galaxies are typically more gas-rich, they require somewhat more violent merger histories to reach the same B/T as a comparable high-mass galaxy (Figures 11-12). To lowest order the gas fractions of progenitor galaxies that contribute to the observed bulge population, and the fraction of bulge mass formed dissipationally (by gas losing angular momentum in mergers and forming stars in concentrated nuclear starbursts) simply reflect the cosmological average gas fractions of progenitor disks corresponding to the same stellar mass and assembly times (Figures 13-14). We have included the effects of gas on merger dynamics because it is known to be very important; however, given the above, our key prediction in this paper specifically would be not be dramatically changed if we ignored these effects throughout.

(6) The predicted major merger rate (mergers per galaxy per Gyr) agrees well with observed merger fractions from $z \sim 0-2$ (Figures 3-5) when one accounts for the observable merger timescale determined by applying the *same* observational methods directly to high-resolution galaxy-galaxy merger simulations (see e.g. Lotz et al. 2008a). The corresponding rate is ~ 0.5 major galaxy-galaxy mergers per central galaxy per unit redshift (in these units, nearly redshift-independent), around $\sim L_*$, and is mass-dependent as per conclusion **(2)**: half to two-thirds of the $\sim L_*$ population has had a major merger since $z \sim 2$, but the fraction is a factor $\sim 3-5$ lower at an order-of-magnitude lower stellar mass, and becomes one (with many galaxies having a couple such mergers) at a factor of a few higher stellar mass (Figures 2 & 6). The merger rate as a function of galaxy-galaxy baryonic mass ratio $\mu_{\rm gal}$, redshift z, and primary stellar mass M_* can be reasonably well fit by the simple functions in Equations 5-10.

(7) Integrating over all mergers, the predicted merger rates yield good agreement with the growth of the mass density in bulge-dominated galaxies, from redshifts $z = 0-1.5$ and (to the extent that color and morphology are correlated) the passive/red sequence population from redshifts $z = 0-4$ (Figure 16). The typical uncertainties in both theory and observations are at the factor ~ 2 level; this is an interesting range discussed below.

7.3. *Robustness*

We have examined how these conclusions depend on a variety of choices, including the empirical HOD constraints, the global cosmology, halo merger rates, substructure tracking, and merger timescales, and find that they are robust (§ 6; Figures 17-18).

Varying the halo occupation model within the range allowed by observations including weak lensing, clustering, group dynamics, and abundance matching methods all yield similar conclusions. A very different halo occupation model, for example simply assuming $M_{\rm gal} \propto M_{\rm halo}$, would yield very different conclusions, but observational constraints are sufficiently tight that within the range allowed, resulting variations are small. Varying the cosmological parameters primarily affects the absolute abundance of halos of a given mass, not e.g. the shape of the merger rate function, and since the observed galaxy mass function is fixed, this difference is simply folded into the halo occupation model and does not change our conclusions.

Halo-halo merger rates, likewise, are sufficiently converged between different simulations such that they yield no large differences. However, a halo-halo merger is not a galaxy-galaxy merger. Typically, one attempts to better approximate the latter by adopting either some merger timescale, representing a delay corresponding to subhalo orbital decay before the galaxy-galaxy merger, or by following subhalos directly in high-resolution cosmological simulations. One can also use galaxy-galaxy mergers identified in cosmological hydrodynamic simulations, after re-normalizing their masses to agree with empirical constraints. Considering variations in each of these choices, we find that they have little effect on the *shape* of the merger rate function, hence little effect on the relative importance of major/minor mergers. Further, some apparent differences in the resulting merger rate owe purely to definitions, and are implicitly normalized out in the HOD. Nevertheless, these different approaches do yield important system-

atic differences in the *absolute* merger rate, at the factor ~ 2 level.

Independent models adopting the halo occupation methodology described here also obtain results in good agreement (see e.g. Zheng et al. 2007; Brown et al. 2008; Pérez-González et al. 2008a; Stewart et al. 2009a). However, models that attempt to predict galaxy formation and merger rates in an a priori manner, such as e.g. cosmological hydrodynamic simulations and semi-analytic models, have reached various mixed conclusions – some in agreement with those here, some not, with significantly larger variation in the predicted galaxy-galaxy merger rates than the factor ~ 2 above (compare e.g. Weinzirl et al. 2009; Parry et al. 2009; Maller et al. 2006; Naab et al. 2007; Governato et al. 2007; Guo & White 2008; Somerville et al. 2008). The origins and implications of these differences is examined in detail in a companion paper (Hopkins et al. 2009f).

However, the important point for our conclusions is that these methods are fundamentally different; they are not strictly tied to observed halo occupation constraints as are the models here. As such, they can yield very different predictions. For example, it is well-known that cosmological simulations without feedback yield efficient star formation at all masses, such that the predicted halo occupation has a form more like $M_{\rm gal} \propto M_{\rm halo}$, and so galaxy-galaxy mergers will, in such a model (without re-normalizing masses) trivially reflect halo-halo mergers. Some semi-analytic models, meanwhile, have well-known discrepancies between predicted and observed populations of satellite galaxies, which propagate to the predicted merger rates. It is increasingly clear that these semi-analytic models have considerable difficulty reproducing the observations of the merger history (generally with the sense that the semi-analytic merger rates/fractions are lower than those observed; see e.g. Jogee et al. 2008; Bertone & Conselice 2009; López-Sanjuan et al. 2009a). In Hopkins et al. (2009f), we show that this indeed primarily owes to well-known mis-matches between the predicted satellite galaxy properties and galaxy mass functions in these models, and those observed. As such, the semi-empirical approach can perform much better in explaining the observations (of course, the model here cannot predict satellite properties as can a semi-analytic model, but that is not its purpose). By adopting the halo occupation constraints directly from observations, the semi-empirical model simply bypasses a major, well-known theoretical uncertainty in attempts to predict merger rates directly from semi-analytic models or cosmological simulations. This does not mean the answer is "built in" implicitly somehow in our models here – what it does mean, however, is that the apparent discrepancy between observations and other predictions of the merger rate owes not to some fundamental problem of ΛCDM, but rather to well-known difficulties in properly modeling the accretion and star-formation histories of galaxies.

Carefully accounting for these distinctions, the different results in various models can be understood. And in fact, despite differences in some quantitative predictions, many of the qualitative conclusions are the same; Parry et al. (2009) and Weinzirl et al. (2009) demonstrate that different SAMs reach similar conclusions regarding how merger rates and the relative importance of major versus minor mergers scale as a function of e.g. galaxy stellar mass and redshift.

7.4. *Outlook and Future Work*

Convergence in predicted merger rates among different theoretical approaches, at the factor ~ 2 level or better, is a remarkable achievement. Unfortunately, obtaining greater convergence in theoretical predictions will be difficult. Applying constraints from empirical halo occupation approaches to e.g. cosmological simulations and semi-analytic models is important. Tighter observational constraints on the halo occupation distribution, in particular at low masses and at high redshifts, will allow semi-empirical models such as those in this paper to greatly extend the dynamic range of predictions (as well as putting strong constraints on a priori models for galaxy formation at these masses and redshifts).

However, we have shown that these differences only account for a fraction of the scatter in theoretical predictions – subtle details of how e.g. halos are defined and followed become important at this level. Moreover resolution limits and the absence of baryons in simulations (which does, at the level of uncertainty here, have potentially important effects on the longevity and merger timescales of subhalos; see e.g. Weinberg et al. 2008) limit all theoretical models. Ideally, high-resolution cosmological hydrodynamic simulations could form the basis for halo occupation models: avoiding ambiguity in identifying a galaxy-galaxy versus halo-halo merger by simply tracking the galaxies (even if their absolute masses are incorrect, and they need to be "repopulated" in post-processing). Although some steps have been made in this direction, it remains prohibitively expensive to simulate large volumes at the desired high resolution with gas physics.

It is also unclear whether a merger rate alone is meaningful at an accuracy much better than a factor ~ 2. At this level, the question of e.g. the "proper" mass ratio becomes important (see e.g. Stewart 2009). What matters, in detail, for galaxy dynamics and the effect of a given merger is a combination of several quantities in the merger "mass ratio" – including stars, gas, and the tightly bound portion of the halo that has been robust to stripping; as such, the halo structure and history, as well as effects such as adiabatic contraction, become important. Moreover, at this level, the orbital parameters, galaxy gas fractions, and progenitor structure (relative bulge-to-disk ratios and disk scale lengths) become non-trivial corrections to the estimate of the effects "per merger." Without models for all of these details, a merger rate constrained to arbitrarily high accuracy does not necessarily translate to a bulge formation model with accuracy better than a similar factor ~ 2.

In the meantime, however, there is considerable room for improvement in the comparison of model predictions and observations of the merger rate. The formal statistical errors in observed merger and close pair fractions are rapidly decreasing; even including cosmic variance, such observations at $z \sim 0-1.2$ are converging to better than a factor of ~ 2. However, as shown in Figure 4, simply putting all such observations on equal footing yields order-of-magnitude scatter; similar uncertainties plague the conversion of these quantities to merger rates (and it is further unclear what the sensitivity is to different mass ratio mergers). This is an area where considerable improvements can and should be made: most of the differences in observational estimates are attributable to different methodologies, observational depth, and selection effects. The conversion of some specific pair or morphologically identified sample to a merger rate should be calibrated to suites of high-resolution N-body simulations, *specifically with mock observations matched to the exact selection and methodology adopted*.

Moreover, the merger rate is predicted to be a non-trivial

function of galaxy mass: many samples identifying merger fractions have ambiguous luminosity selection; what is ultimately necessary are samples with well-defined stellar or baryonic mass selection. At the level of present data quality and theoretical convergence, order-of-magnitude estimates of merger lifetimes and lack of such calibration represent the dominant uncertainty in comparisons.

Improvements are being made in this area: Lotz et al. (2008a) have calibrated the merger timescale for major pair samples of different separations and certain specific automated morphological selection criteria to mock observations of high-resolution hydrodynamic merger simulations. Conselice et al. (2009) adopt these and similar detailed calibrations to attempt to address consistency between merger populations identified with different methodologies. Jogee et al. (2008, 2009) attempt to calibrate their morphological selection criteria as a function of merger mass ratio. Various works have attempted to quantify merger rates as a function of stellar mass, rather than in a pure magnitude-limited sample (see e.g. Bell et al. 2006a; Conselice et al. 2008; Bundy et al. 2009; López-Sanjuan et al. 2009b; Darg et al. 2009b).

Together, these approaches will allow rigorous comparison of predicted and observed galaxy-galaxy merger rates as a function of galaxy stellar mass, redshift, and (ideally) mass ratio. Obviously, extension of observational constraints in any of this parameter space represents a valuable constraint on the models here. Using the calibrations above, we attempt such a comparison specific to different observational methods (at least in terms of pair versus morphological fractions), and find good agreement between predicted and observed merger rates, and the integrated buildup of the bulge population. Considering the most well-constrained observations and well-calibrated conversions, we find agreement within a similar factor ~ 2 as that characteristic of the theoretical uncertainties.

Far from implying that the problem is "solved," such a factor of ~ 2 is of great interest. There is a large parameter space where predicted merger rates are consistent with observed merger/pair fractions as a function of mass and redshift and can be tuned to precisely account for the entire bulge mass budget of the Universe. However, allowing for the factor ~ 2 uncertainty in one direction would lead to "too many" mergers, implying that mergers must be less efficient than cosmologically predicted: this might mean that real gas fractions are in fact higher than what we have modeled here, or that tidal destruction of satellites is efficient, even in the major merger regime, or that there is some problem in our understanding of halo occupation statistics or cosmological dark matter merger rates.

On the other hand, allowing for the same factor of ~ 2 variation in the opposite sense would imply that $\sim$half the bulge mass density of the Universe could not be attributed to mergers as we understand them. This means that, within the present uncertainties, secular processes such as bar or disk instabilities might account for up to half of the bulge mass of the Universe. Since the uncertainties grow at low mass, the fraction could be even higher at lower masses.

Independent observational tests can put complementary constraints on these possibilities. It must be emphasized, for example, that essentially all numerical studies of spheroid kinematics find that *only* mergers can reproduce the observed kinematic properties of observed elliptical galaxies and "classical" bulges (Hernquist 1989, 1992, 1993; Barnes 1988, 1992; Schweizer 1992; Bournaud et al. 2005; Naab et al. 2006; Naab & Trujillo 2006; Cox et al. 2006a; Jesseit et al. 2007). These are, in general, the bulges whose formation history we predict here. Disk instabilities and secular evolution (e.g. bar instabilities, harassment, and other isolated modes) can indeed produce bulges, but these are "pseudobulges" (Pfenniger 1984; Combes et al. 1990; Raha et al. 1991; Kuijken & Merrifield 1995; O'Neill & Dubinski 2003; Athanassoula 2005), with clearly distinct shapes, kinematics, structural properties, and colors from classical bulges (for a review, see Kormendy & Kennicutt 2004).

Observations at present indicate that pseudobulges constitute only a small fraction of the total mass density in spheroids ($\lesssim 10\%$; see Allen et al. 2006; Ball et al. 2006; Driver et al. 2007); they do, however, become a large fraction of the bulge population in small bulges in late-type hosts (e.g. Sb/c, corresponding to typical $M_{\rm gal} \lesssim 10^{10}\,M_{\odot}$; see Carollo et al. 1998; Kormendy & Kennicutt 2004, and references therein). However, this is not to say that secular processes cannot, in principle, build some massive bulges (see e.g. Debattista et al. 2004, 2006). And it is not clear that mergers – specifically minor mergers with mass ratios $\mu_{\rm gal} \lesssim 1/10$ – cannot build pseudobulges, depending on e.g. the structural properties of the secondary and orbital parameters of the merger (see e.g. Gauthier et al. 2006; Younger et al. 2008a; Eliche-Moral et al. 2008).

Improvements in theoretical constraints (from high-resolution simulations) on how bulges with different structural properties are formed, combined with improved observational constraints on the distribution of these structural properties, can constrain the role of secular processes at better than a factor ~ 2 level (at least at low redshifts) – a level at which theoretical models cannot yet uniquely predict the importance of mergers. On the other hand, observational constraints on the mass budget in extended galaxy halos, intra-group and intra-cluster light can constrain satellite disruption (see e.g. Lin & Mohr 2004; Cypriano et al. 2006; Brown et al. 2008; Laganá et al. 2008), and observations of high redshift disk+bulge systems that may represent recent re-forming or relaxing merger remnants can constrain the efficiency of bulge formation in mergers (Hammer et al. 2005; Zheng et al. 2005; Trujillo & Pohlen 2005; Flores et al. 2006; Puech et al. 2007a,b, 2008; Atkinson et al. 2007). Together, these improvements in observational constraints and theoretical models have the potential to enable precision tests of models for bulge formation in mergers, and allow a robust determination of the relative roles of secular processes, minor mergers, and major mergers in galaxy formation, as a function of cosmic time and galaxy properties.

In order to facilitate comparison with future observations, we have provided fitting functions to both the predicted merger rates as a function of galaxy mass and mass ratio, and to the relative contributions of these mergers to bulge formation. However, for various applications, additional information is desired. We therefore make public a simple "merger rate calculator" code[25] which can be used to obtain the predicted merger rates from the models as a function of e.g. galaxy mass, mass ratio, redshift, and galaxy gas fractions. The script can be used to determine merger rates as a function of halo, stellar, or total galaxy baryonic masses, and can be used to restrict to e.g. gas-rich ("wet") or gas-poor ("dry")

[25] http://www.cfa.harvard.edu/~phopkins/Site/mergercalc.html

mergers. It also allows for different choices with respect to e.g. the stellar mass functions used to normalize the HOD and $M_{\rm gal}(M_{\rm halo})$ distribution used in the models here, and different cosmological parameters. As desired, it can output the merger rate per galaxy, the volumetric total merger rate (mergers per unit volume per unit time), or merger fractions with the appropriate observable timescales used here as calibrated for pair or morphologically-selected samples. We note that, in the interest of running time and memory use, the script uses some of fitting functions and approximations to the full models discussed here – however, we have tested extensively that the approximations and fitting functions used yield much smaller differences in the ultimate merger rates than the inherent uncertainties discussed here.

We thank Andrew Benson, Owen Parry, Simon White, Volker Springel, Gabriella de Lucia, and Carlos Frenk for helpful discussions. Support for PFH was provided by the Miller Institute for Basic Research in Science, University of California Berkeley. JDY acknowledges support from NASA through Hubble Fellowship grant HST-HF-01243.01 awarded by the Space Telescope Science Institute, which is operated by the Association of Universities for Research in Astronomy, Inc., for NASA, under contract NAS 5-26555.

REFERENCES

Abraham, R. G., et al. 2007, ApJ, 669, 184
Alexander, D. M., Smail, I., Bauer, F. E., Chapman, S. C., Blain, A. W., Brandt, W. N., & Ivison, R. J. 2005, Nature, 434, 738
Allen, P. D., Driver, S. P., Graham, A. W., Cameron, E., Liske, J., & de Propris, R. 2006, MNRAS, 371, 2
Aller, M. C., & Richstone, D. O. 2007, ApJ, 665, 120
Athanassoula, E. 2005, MNRAS, 358, 1477
Atkinson, N., Conselice, C. J., & Fox, N. 2007, MNRAS, in press, arXiv:0712.1316 [astro-ph]
Avila-Reese, V., Zavala, J., Firmani, C., & Hernández-Toledo, H. M. 2008, AJ, 136, 1340
Ball, N. M., Loveday, J., Brunner, R. J., Baldry, I. K., & Brinkmann, J. 2006, MNRAS, 373, 845
Barnes, J. E. 1988, ApJ, 331, 699
—. 1992, ApJ, 393, 484
Barnes, J. E., & Hernquist, L. 1992, ARA&A, 30, 705
—. 1996, ApJ, 471, 115
Barnes, J. E., & Hernquist, L. E. 1991, ApJ, 370, L65
Barton, E. J., Arnold, J. A., Zentner, A. R., Bullock, J. S., & Wechsler, R. H. 2007, ApJ, 671, 1538
Behroozi, P. S., Conroy, C., & Wechsler, R. H. 2010, ApJ, in press, arXiv:1001.0015
Bell, E. F., & de Jong, R. S. 2000, MNRAS, 312, 497
—. 2001, ApJ, 550, 212
Bell, E. F., McIntosh, D. H., Katz, N., & Weinberg, M. D. 2003, ApJS, 149, 289
Bell, E. F., Phleps, S., Somerville, R. S., Wolf, C., Borch, A., & Meisenheimer, K. 2006a, ApJ, 652, 270
Bell, E. F., et al. 2005, ApJ, 625, 23
—. 2006b, ApJ, 640, 241
Bennert, N., Canalizo, G., Jungwiert, B., Stockton, A., Schweizer, F., Peng, C. Y., & Lacy, M. 2008, ApJ, 677, 846
Benson, A. J. 2005, MNRAS, 358, 551
Benson, A. J., Lacey, C. G., Frenk, C. S., Baugh, C. M., & Cole, S. 2004, MNRAS, 351, 1215
Bertone, S., & Conselice, C. J. 2009, MNRAS, 396, 2345
Binney, J., & Tremaine, S. 1987, Galactic dynamics (Princeton, NJ, Princeton University Press, 1987)
Blain, A. W., Jameson, A., Smail, I., Longair, M. S., Kneib, J.-P., & Ivison, R. J. 1999, MNRAS, 309, 715
Bluck, A. F. L., Conselice, C. J., Bouwens, R. J., Daddi, E., Dickinson, M., Papovich, C., & Yan, H. 2009, MNRAS, 394, L51
Borch, A., et al. 2006, A&A, 453, 869
Borriello, A., & Salucci, P. 2001, MNRAS, 323, 285
Bouché, N., et al. 2007, ApJ, 671, 303
Bournaud, F., Jog, C. J., & Combes, F. 2005, A&A, 437, 69
Bower, R. G., Benson, A. J., Malbon, R., Helly, J. C., Frenk, C. S., Baugh, C. M., Cole, S., & Lacey, C. G. 2006, MNRAS, 370, 645
Boylan-Kolchin, M., Ma, C.-P., & Quataert, E. 2008, MNRAS, 383, 93
Bridge, C. R., Carlberg, R. G., & Sullivan, M. 2010, ApJ, 709, 1067
Bridge, C. R., et al. 2007, ApJ, 659, 931
Brough, S., Forbes, D. A., Kilborn, V. A., & Couch, W. 2006, MNRAS, 370, 1223
Brown, M. J. I., Dey, A., Jannuzi, B. T., Brand, K., Benson, A. J., Brodwin, M., Croton, D. J., & Eisenhardt, P. R. 2007, ApJ, 654, 858
Brown, M. J. I., et al. 2008, ApJ, 682, 937
Bundy, K., Ellis, R. S., & Conselice, C. J. 2005, ApJ, 625, 621
Bundy, K., Fukugita, M., Ellis, R. S., Targett, T. A., Belli, S., & Kodama, T. 2009, ApJ, 697, 1369
Bundy, K., et al. 2006, ApJ, 651, 120
Burkert, A., Naab, T., Johansson, P. H., & Jesseit, R. 2008, ApJ, 685, 897
Calura, F., Jimenez, R., Panter, B., Matteucci, F., & Heavens, A. F. 2008, ApJ, 682, 252
Canalizo, G., & Stockton, A. 2001, ApJ, 555, 719
Carollo, C. M., Stiavelli, M., & Mack, J. 1998, AJ, 116, 68
Cassata, P., et al. 2005, MNRAS, 357, 903
Chabrier, G. 2003, PASP, 115, 763
Combes, F., Debbasch, F., Friedli, D., & Pfenniger, D. 1990, A&A, 233, 82
Conroy, C., & Wechsler, R. H. 2009, ApJ, 696, 620
Conroy, C., Wechsler, R. H., & Kravtsov, A. V. 2006, ApJ, 647, 201
Conroy, C., et al. 2007, ApJ, 654, 153
Conselice, C. J. 2009, MNRAS, in press [arXiv:0906.4704]
Conselice, C. J., Bershady, M. A., Dickinson, M., & Papovich, C. 2003, AJ, 126, 1183
Conselice, C. J., Rajgor, S., & Myers, R. 2008, MNRAS, 386, 909
Conselice, C. J., Yang, C., & Bluck, A. F. L. 2009, MNRAS, 394, 1956
Cooray, A. 2005, MNRAS, 364, 303
—. 2006, MNRAS, 365, 842
Cox, T. J., Dutta, S. N., Di Matteo, T., Hernquist, L., Hopkins, P. F., Robertson, B., & Springel, V. 2006a, ApJ, 650, 791
Cox, T. J., Jonsson, P., Primack, J. R., & Somerville, R. S. 2006b, MNRAS, 373, 1013
Cox, T. J., Jonsson, P., Somerville, R. S., Primack, J. R., & Dekel, A. 2008, MNRAS, 384, 386
Cresci, G., et al. 2009, ApJ, 697, 115
Croton, D. J., et al. 2006, MNRAS, 365, 11
Cypriano, E. S., Sodré, L. J., Campusano, L. E., Dale, D. A., & Hardy, E. 2006, AJ, 131, 2417
Daddi, E., et al. 2005, ApJ, 626, 680
Damen, M., Labbé, I., Franx, M., van Dokkum, P. G., Taylor, E. N., & Gawiser, E. J. 2009, ApJ, 690, 937
Darg, D. W., et al. 2009a, MNRAS, in press, arXiv:0903.4937
—. 2009b, MNRAS, in press, arXiv:0903.5057
Dasyra, K. M., et al. 2006, ApJ, 638, 745
—. 2007, ApJ, 657, 102
de Lucia, G., & Blaizot, J. 2007, MNRAS, 375, 2
De Lucia, G., Kauffmann, G., Springel, V., White, S. D. M., Lanzoni, B., Stoehr, F., Tormen, G., & Yoshida, N. 2004, MNRAS, 348, 333
De Propris, R., Liske, J., Driver, S. P., Allen, P. D., & Cross, N. J. G. 2005, AJ, 130, 1516
de Ravel, L., et al. 2009, A&A, 498, 379
Debattista, V. P., Carollo, C. M., Mayer, L., & Moore, B. 2004, ApJ, 604, L93
Debattista, V. P., Mayer, L., Carollo, C. M., Moore, B., Wadsley, J., & Quinn, T. 2006, ApJ, 645, 209
di Matteo, P., Combes, F., Melchior, A.-L., & Semelin, B. 2007, A&A, 468, 61
Di Matteo, T., Springel, V., & Hernquist, L. 2005, Nature, 433, 604
Doyon, R., Wells, M., Wright, G. S., Joseph, R. D., Nadeau, D., & James, P. A. 1994, ApJ, 437, L23
Driver, S. P., Allen, P. D., Liske, J., & Graham, A. W. 2007, ApJ, 657, L85
Eke, V. R., et al. 2004, MNRAS, 355, 769
Elahi, P. J., Thacker, R. J., Widrow, L. M., & Scannapieco, E. 2008, MNRAS, in press, arXiv:0811.0206 [astro-ph]

Eliche-Moral, M. C., González-García, A. C., Balcells, M., Aguerri, J. A. L., Gallego, J., & Zamorano, J. 2008, in Astronomical Society of the Pacific Conference Series, Vol. 396, Astronomical Society of the Pacific Conference Series, ed. J. G. Funes & E. M. Corsini, 359–+
Erb, D. K. 2008, ApJ, 674, 151
Erb, D. K., Steidel, C. C., Shapley, A. E., Pettini, M., Reddy, N. A., & Adelberger, K. L. 2006, ApJ, 646, 107
Fakhouri, O., & Ma, C.-P. 2008a, MNRAS, in press, arXiv:0808.2471 [astro-ph]
—. 2008b, MNRAS, 386, 577
Ferrarese, L., & Merritt, D. 2000, ApJ, 539, L9
Flores, H., Hammer, F., Puech, M., Amram, P., & Balkowski, C. 2006, A&A, 455, 107
Fontana, A., et al. 2004, A&A, 424, 23
—. 2006, A&A, 459, 745
Forster Schreiber, N. M., et al. 2009, ApJ, 706, 1364
Foster, C., Proctor, R. N., Forbes, D. A., Spolaor, M., Hopkins, P. F., & Brodie, J. P. 2009, MNRAS, 1562
Franceschini, A., et al. 2006, A&A, 453, 397
Franx, M., van Dokkum, P. G., Schreiber, N. M. F., Wuyts, S., Labbé, I., & Toft, S. 2008, ApJ, 688, 770
Gao, L., White, S. D. M., Jenkins, A., Stoehr, F., & Springel, V. 2004, MNRAS, 355, 819
Gauthier, J.-R., Dubinski, J., & Widrow, L. M. 2006, ApJ, 653, 1180
Gebhardt, K., et al. 2000, ApJ, 539, L13
Genel, S., Genzel, R., Bouché, N., Naab, T., & Sternberg, A. 2008, ApJ, in press, arXiv:0812.3154
Genzel, R., Tacconi, L. J., Rigopoulou, D., Lutz, D., & Tecza, M. 2001, ApJ, 563, 527
Genzel, R., et al. 2008, ApJ, 687, 59
Gerke, B. F., et al. 2007, MNRAS, 222
Gottlöber, S., Klypin, A., & Kravtsov, A. V. 2001, ApJ, 546, 223
Governato, F., Willman, B., Mayer, L., Brooks, A., Stinson, G., Valenzuela, O., Wadsley, J., & Quinn, T. 2007, MNRAS, 374, 1479
Governato, F., et al. 2008, MNRAS, in press, arXiv:0812.0379 [astro-ph]
Grazian, A., et al. 2007, A&A, 465, 393
Guo, Q., & White, S. D. M. 2008, MNRAS, 384, 2
Guyon, O., Sanders, D. B., & Stockton, A. 2006, ApJS, 166, 89
Hammer, F., Flores, H., Elbaz, D., Zheng, X. Z., Liang, Y. C., & Cesarsky, C. 2005, A&A, 430, 115
Hernquist, L. 1989, Nature, 340, 687
—. 1992, ApJ, 400, 460
—. 1993, ApJ, 409, 548
Hoffman, L. K., Cox, T. J., Dutta, S. N., & Hernquist, L. E. 2009, ApJ, in press, arXiv:0903.3064 [astro-ph]
Hopkins, A. M., & Beacom, J. F. 2006, ApJ, 651, 142
Hopkins, P. F., Bundy, K., Hernquist, L., & Ellis, R. S. 2007a, ApJ, 659, 976
Hopkins, P. F., Cox, T. J., Dutta, S. N., Hernquist, L., Kormendy, J., & Lauer, T. R. 2009a, ApJS, 181, 135
Hopkins, P. F., Cox, T. J., & Hernquist, L. 2008a, ApJ, 689, 17
Hopkins, P. F., Cox, T. J., Kereš, D., & Hernquist, L. 2008b, ApJS, 175, 390
Hopkins, P. F., Cox, T. J., Younger, J. D., & Hernquist, L. 2009b, ApJ, 691, 1168
Hopkins, P. F., & Hernquist, L. 2006, ApJS, 166, 1
—. 2009, ApJ, 694, 599
Hopkins, P. F., Hernquist, L., Cox, T. J., Di Matteo, T., Martini, P., Robertson, B., & Springel, V. 2005a, ApJ, 630, 705
Hopkins, P. F., Hernquist, L., Cox, T. J., Dutta, S. N., & Rothberg, B. 2008c, ApJ, 679, 156
Hopkins, P. F., Hernquist, L., Cox, T. J., & Kereš, D. 2008d, ApJS, 175, 356
Hopkins, P. F., Hernquist, L., Cox, T. J., Kereš, D., & Wuyts, S. 2009c, ApJ, 691, 1424
Hopkins, P. F., Hernquist, L., Cox, T. J., Robertson, B., & Krause, E. 2007b, ApJ, 669, 45
—. 2007c, ApJ, 669, 67
Hopkins, P. F., Hernquist, L., Cox, T. J., Younger, J. D., & Besla, G. 2008e, ApJ, 688, 757
Hopkins, P. F., Hernquist, L., Martini, P., Cox, T. J., Robertson, B., Di Matteo, T., & Springel, V. 2005b, ApJ, 625, L71
Hopkins, P. F., Hickox, R., Quataert, E., & Hernquist, L. 2009d, MNRAS, 398, 333
Hopkins, P. F., Lauer, T. R., Cox, T. J., Hernquist, L., & Kormendy, J. 2009e, ApJS, 181, 486
Hopkins, P. F., Lidz, A., Hernquist, L., Coil, A. L., Myers, A. D., Cox, T. J., & Spergel, D. N. 2007d, ApJ, 662, 110
Hopkins, P. F., Richards, G. T., & Hernquist, L. 2007e, ApJ, 654, 731
Hopkins, P. F., et al. 2009f, MNRAS, in preparation
—. 2009g, MNRAS, 397, 802
Ilbert, O., et al. 2009, ApJ, in press, arXiv:0903.0102
James, P., Bate, C., Wells, M., Wright, G., & Doyon, R. 1999, MNRAS, 309, 585
Jesseit, R., Cappellari, M., Naab, T., Emsellem, E., & Burkert, A. 2009, MNRAS, 397, 1202
Jesseit, R., Naab, T., Peletier, R. F., & Burkert, A. 2007, MNRAS, 376, 997
Jiang, C. Y., Jing, Y. P., Faltenbacher, A., Lin, W. P., & Li, C. 2008, ApJ, 675, 1095
Jogee, S., Scoville, N., & Kenney, J. D. P. 2005, ApJ, 630, 837
Jogee, S., et al. 2008, in Astronomical Society of the Pacific Conference Series, Vol. 396, Astronomical Society of the Pacific Conference Series, ed. J. G. Funes & E. M. Corsini, 337–+
Jogee, S., et al. 2009, ApJ, 697, 1971
Joseph, R. D., & Wright, G. S. 1985, MNRAS, 214, 87
Kajisawa, M., et al. 2009, ApJ, 702, 1393
Kannappan, S. J. 2004, ApJ, 611, L89
Kartaltepe, J. S., et al. 2007, ApJS, 172, 320
Kazantzidis, S., Bullock, J. S., Zentner, A. R., Kravtsov, A. V., & Moustakas, L. A. 2008, ApJ, 688, 254
Kazantzidis, S., Zentner, A. R., Kravtsov, A. V., Bullock, J. S., & Debattista, V. P. 2009, ApJ, in press, arXiv:0902.1983 [astro-ph]
Khochfar, S., & Burkert, A. 2006, A&A, 445, 403
Khochfar, S., & Silk, J. 2006, ApJ, 648, L21
—. 2008, ArXiv e-prints
Kitzbichler, M. G., & White, S. D. M. 2008, MNRAS, 391, 1489
Komatsu, E., et al. 2009, ApJS, 180, 330
Kormendy, J., Fisher, D. B., Cornell, M. E., & Bender, R. 2009, ApJS, 182, 216
Kormendy, J., & Kennicutt, Jr., R. C. 2004, ARA&A, 42, 603
Kravtsov, A. V., Berlind, A. A., Wechsler, R. H., Klypin, A. A., Gottlöber, S., Allgood, B., & Primack, J. R. 2004, ApJ, 609, 35
Kriek, M., et al. 2006, ApJ, 649, L71
Krivitsky, D. S., & Kontorovich, V. M. 1997, A&A, 327, 921
Kuijken, K., & Merrifield, M. R. 1995, ApJ, 443, L13
Labbé, I., et al. 2005, ApJ, 624, L81
Laganá, T. F., Lima Neto, G. B., Andrade-Santos, F., & Cypriano, E. S. 2008, A&A, 485, 633
Lake, G., & Dressler, A. 1986, ApJ, 310, 605
Lauer, T. R., et al. 2007, ApJ, 664, 226
Lee, K., Giavalisco, M., Conroy, C., Wechsler, R. H., Ferguson, H. C., Somerville, R. S., Dickinson, M. E., & Urry, C. M. 2009, ApJ, 695, 368
Lin, L., et al. 2004, ApJ, 617, L9
—. 2008, ApJ, 681, 232
Lin, Y.-T., & Mohr, J. J. 2004, ApJ, 617, 879
López-Sanjuan, C., Balcells, M., Pérez-González, P. G., Barro, G., García-Dabó, C. E., Gallego, J., & Zamorano, J. 2009a, A&A, in press [arXiv:0905.2765]
López-Sanjuan, C., et al. 2009b, ApJ, 694, 643
Lotz, J. M., Jonsson, P., Cox, T. J., & Primack, J. R. 2008a, MNRAS, 391, 1137
—. 2009a, MNRAS, in press, arXiv:0912.1593
—. 2009b, MNRAS, in press, arXiv:0912.1590
Lotz, J. M., Madau, P., Giavalisco, M., Primack, J., & Ferguson, H. C. 2006, ApJ, 636, 592
Lotz, J. M., Primack, J., & Madau, P. 2004, AJ, 128, 163
Lotz, J. M., et al. 2008b, ApJ, 672, 177
Magorrian, J., et al. 1998, AJ, 115, 2285
Makino, J., & Hut, P. 1997, ApJ, 481, 83
Malin, D. F., & Carter, D. 1980, Nature, 285, 643
—. 1983, ApJ, 274, 534
Maller, A. H., Katz, N., Kereš, D., Davé, R., & Weinberg, D. H. 2006, ApJ, 647, 763
Mamon, G. A. 2006, in Groups of Galaxies in the Nearby Universe, ed. I. Saviane, V. Ivanov, & J. Borissova
Mandelbaum, R., Seljak, U., Kauffmann, G., Hirata, C. M., & Brinkmann, J. 2006, MNRAS, 368, 715
Mannucci, F., et al. 2009, MNRAS, 398, 1915
Marchesini, D., van Dokkum, P. G., Förster Schreiber, N. M., Franx, M., Labbé, I., & Wuyts, S. 2009, ApJ, 701, 1765
Martin, D. C., et al. 2007, ApJS, 173, 415
McGaugh, S. S. 2005, ApJ, 632, 859
Mihos, J. C., & Hernquist, L. 1994a, ApJ, 427, 112
—. 1994b, ApJ, 431, L9
—. 1996, ApJ, 464, 641

Moster, B. P., Somerville, R. S., Maulbetsch, C., van den Bosch, F. C., Maccio', A. V., Naab, T., & Oser, L. 2009, ApJ, in press, arXiv:0903.4682 [astro-ph]
Naab, T., & Burkert, A. 2003, ApJ, 597, 893
Naab, T., Jesseit, R., & Burkert, A. 2006, MNRAS, 372, 839
Naab, T., Johansson, P. H., & Ostriker, J. P. 2009, ApJ, 699, L178
Naab, T., Johansson, P. H., Ostriker, J. P., & Efstathiou, G. 2007, ApJ, 658, 710
Naab, T., & Trujillo, I. 2006, MNRAS, 369, 625
Neistein, E., van den Bosch, F. C., & Dekel, A. 2006, MNRAS, 372, 933
Noeske, K. G., et al. 2007a, ApJ, 660, L47
—. 2007b, ApJ, 660, L43
Nurmi, P., Heinämäki, P., Saar, E., Einasto, M., Holopainen, J., Martínez, V. J., & Einasto, J. 2006, A&A, in press [astro-ph/0611941]
Okamoto, T., Eke, V. R., Frenk, C. S., & Jenkins, A. 2005, MNRAS, 363, 1299
O'Neill, J. K., & Dubinski, J. 2003, MNRAS, 346, 251
Pannella, M., Hopp, U., Saglia, R. P., Bender, R., Drory, N., Salvato, M., Gabasch, A., & Feulner, G. 2006, ApJ, 639, L1
Papovich, C., et al. 2006, ApJ, 640, 92
Parry, O. H., Eke, V. R., & Frenk, C. S. 2009, MNRAS, 396, 1972
Patton, D. R., & Atfield, J. E. 2008, ApJ, 685, 235
Patton, D. R., et al. 2002, ApJ, 565, 208
Pérez-González, P. G., Trujillo, I., Barro, G., Gallego, J., Zamorano, J., & Conselice, C. J. 2008a, ApJ, 687, 50
Pérez-González, P. G., et al. 2008b, ApJ, 675, 234
Persic, M., & Salucci, P. 1988, MNRAS, 234, 131
Persic, M., Salucci, P., & Stel, F. 1996, MNRAS, 281, 27
Pfenniger, D. 1984, A&A, 134, 373
Puech, M., Hammer, F., Flores, H., Neichel, B., Yang, Y., & Rodrigues, M. 2007a, A&A, 476, L21
Puech, M., Hammer, F., Lehnert, M. D., & Flores, H. 2007b, A&A, 466, 83
Puech, M., et al. 2008, A&A, 484, 173
Purcell, C. W., Kazantzidis, S., & Bullock, J. S. 2009, ApJ, 694, L98
Quinn, P. J., & Goodman, J. 1986, ApJ, 309, 472
Raha, N., Sellwood, J. A., James, R. A., & Kahn, F. D. 1991, Nature, 352, 411
Robertson, B., Bullock, J. S., Cox, T. J., Di Matteo, T., Hernquist, L., Springel, V., & Yoshida, N. 2006, ApJ, 645, 986
Robertson, B. E., & Bullock, J. S. 2008, ApJ, 685, L27
Rothberg, B., & Joseph, R. D. 2004, AJ, 128, 2098
—. 2006a, AJ, 131, 185
—. 2006b, AJ, 132, 976
Ruhland, C., Bell, E. F., Haeussler, B., Taylor, E. N., Barden, M., & McIntosh, D. H. 2009, ApJ, in press, arXiv:0901.4340 [astro-ph]
Salucci, P., Szuszkiewicz, E., Monaco, P., & Danese, L. 1999, MNRAS, 307, 637
Sanders, D. B., & Mirabel, I. F. 1996, ARA&A, 34, 749
Sanders, D. B., Soifer, B. T., Elias, J. H., Madore, B. F., Matthews, K., Neugebauer, G., & Scoville, N. Z. 1988, ApJ, 325, 74
Scannapieco, C., Tissera, P. B., White, S. D. M., & Springel, V. 2008, MNRAS, 389, 1137
Schweizer, F. 1980, ApJ, 237, 303
—. 1982, ApJ, 252, 455
Schweizer, F. 1992, in Physics of Nearby Galaxies: Nature or Nurture?, ed. T. X. Thuan, C. Balkowski, & J. Tran Thanh van, 283–+
—. 1996, AJ, 111, 109
Schweizer, F., & Seitzer, P. 1992, AJ, 104, 1039
Shankar, F., Weinberg, D. H., & Miralda-Escudé, J. 2009, ApJ, 690, 20
Shapiro, K. L., et al. 2008, ApJ, 682, 231
Shapley, A. E., Coil, A. L., Ma, C.-P., & Bundy, K. 2005, ApJ, 635, 1006
Sheth, R. K., Mo, H. J., & Tormen, G. 2001, MNRAS, 323, 1
Shier, L. M., & Fischer, J. 1998, ApJ, 497, 163
Soifer, B. T., et al. 1984a, ApJ, 278, L71
—. 1984b, ApJ, 283, L1
Soltan, A. 1982, MNRAS, 200, 115
Somerville, R. S., Hopkins, P. F., Cox, T. J., Robertson, B. E., & Hernquist, L. 2008, MNRAS, 391, 481
Spergel, D. N., et al. 2003, ApJS, 148, 175
—. 2007, ApJS, 170, 377
Springel, V., Di Matteo, T., & Hernquist, L. 2005a, ApJ, 620, L79
—. 2005b, MNRAS, 361, 776
Springel, V., Frenk, C. S., & White, S. D. M. 2006, Nature, 440, 1137
Springel, V., & Hernquist, L. 2005, ApJ, 622, L9
Springel, V., et al. 2005c, Nature, 435, 629
Stewart, K. R. 2009, To appear in proceedings of "Galaxy Evolution: Emerging Insights and Future Challenges", arXiv:0902.2214
Stewart, K. R., Bullock, J. S., Barton, E. J., & Wechsler, R. H. 2009a, ApJ, 702, 1005
Stewart, K. R., Bullock, J. S., Wechsler, R. H., & Maller, A. H. 2009b, ApJ, 702, 307
Stewart, K. R., Bullock, J. S., Wechsler, R. H., Maller, A. H., & Zentner, A. R. 2008, ApJ, 683, 597
Tacconi, L. J., Genzel, R., Lutz, D., Rigopoulou, D., Baker, A. J., Iserlohe, C., & Tecza, M. 2002, ApJ, 580, 73
Tacconi, L. J., et al. 2008, ApJ, 680, 246
—. 2010, Nature, in press, arXiv:1002.2149
Tinker, J. L., Weinberg, D. H., Zheng, Z., & Zehavi, I. 2005, ApJ, 631, 41
Toft, S., et al. 2007, ApJ, 671, 285
Toomre, A. 1977, in Evolution of Galaxies and Stellar Populations (New Haven: Yale University Observatory), ed. B. M. Tinsley & R. B. Larson, 401
Trujillo, I., Conselice, C. J., Bundy, K., Cooper, M. C., Eisenhardt, P., & Ellis, R. S. 2007, MNRAS, 382, 109
Trujillo, I., & Pohlen, M. 2005, ApJ, 630, L17
Vale, A., & Ostriker, J. P. 2006, MNRAS, 371, 1173
van den Bosch, F. C., Tormen, G., & Giocoli, C. 2005, MNRAS, 359, 1029
van den Bosch, F. C., et al. 2007, MNRAS, 376, 841
van Dokkum, P. G. 2005, AJ, 130, 2647
van Dokkum, P. G., et al. 2006, ApJ, 638, L59
Wang, L., Li, C., Kauffmann, G., & de Lucia, G. 2006, MNRAS, 371, 537
Weil, M. L., & Hernquist, L. 1994, ApJ, 431, L79
—. 1996, ApJ, 460, 101
Weinberg, D. H., Colombi, S., Davé, R., & Katz, N. 2008, ApJ, 678, 6
Weinmann, S. M., van den Bosch, F. C., Yang, X., & Mo, H. J. 2006a, MNRAS, 366, 2
Weinmann, S. M., van den Bosch, F. C., Yang, X., Mo, H. J., Croton, D. J., & Moore, B. 2006b, MNRAS, 372, 1161
Weinzirl, T., Jogee, S., Khochfar, S., Burkert, A., & Kormendy, J. 2009, ApJ, 696, 411
Wetzel, A. R. 2010, MNRAS, in press, arXiv:1001.4792
Wetzel, A. R., Cohn, J. D., & White, M. 2009a, MNRAS, 395, 1376
—. 2009b, MNRAS, 281
White, S. D. M. 1976, MNRAS, 174, 467
White, S. D. M., & Rees, M. J. 1978, MNRAS, 183, 341
Wolf, C., et al. 2005, ApJ, 630, 771
Woods, D. F., & Geller, M. J. 2007, AJ, 134, 527
Woods, D. F., Geller, M. J., & Barton, E. J. 2006, AJ, 132, 197
Xu, C. K., Sun, Y. C., & He, X. T. 2004, ApJ, 603, L73
Yan, R., Madgwick, D. S., & White, M. 2003, ApJ, 598, 848
Yang, X., Mo, H. J., Jing, Y. P., & van den Bosch, F. C. 2005, MNRAS, 358, 217
Younger, J. D., Hopkins, P. F., Cox, T. J., & Hernquist, L. 2008a, ApJ, 686, 815
Younger, J. D., et al. 2008b, ApJ, 688, 59
Yu, Q., & Tremaine, S. 2002, MNRAS, 335, 965
Zentner, A. R., Berlind, A. A., Bullock, J. S., Kravtsov, A. V., & Wechsler, R. H. 2005, ApJ, 624, 505
Zheng, X. Z., Hammer, F., Flores, H., Assémat, F., & Rawat, A. 2005, A&A, 435, 507
Zheng, Z., Coil, A. L., & Zehavi, I. 2007, ApJ, 667, 760